Ceramic Finishing Company

State College, Pennsylvania

TECHNICAL REPORT NO. 8

STRENGTHENING OXIDES BY REDUCTION OF CRYSTAL ANISOTROPY

APRIL, 1972

Prepared by:

Henry P. Kirchner

Robert M. Gruver

Prepared under Contract No. N00014-66-C0190 for the Office of Naval Research, Department of the Navy, Requisition Number NR032-498

Security Classification

DOCUMENT CONTROL DATA - R & D

(Security classification of title, body of abstract and indexing annotation must be entered when the overall report is classified)

1. ORIGINATING ACTIVITY (Corporate author)	2a. REPORT SECURITY CLASSIFICATION
Ceramic Finishing Company	Unclassified
	2b. GROUP

3. REPORT TITLE

Strengthening Oxides by Reduction of Crystal Anisotropy

4. DESCRIPTIVE NOTES (Type of report and inclusive dates)

Technical Report No. 6

5. AUTHOR(S) (First name, middle initial, last name)

Kirchner, Henry P.

Gruver, Robert M.

6. REPORT DATE	7a. TOTAL NO. OF PAGES	7b. NO. OF REFS
April, 1972	83	47

8a. CONTRACT OR GRANT NO.	9a. ORIGINATOR'S REPORT NUMBER(S)
N00014-66-C0190	
b. PROJECT NO. Requisition Number	
c. NR 032-498	9b. OTHER REPORT NO(S) (Any other numbers that may be assigned this report)
d.	

10. DISTRIBUTION STATEMENT

Distribution of this report is unlimited.

11. SUPPLEMENTARY NOTES	12. SPONSORING MILITARY ACTIVITY
	Office of Naval Research Department of the Navy

13. ABSTRACT

In single phase polycrystalline ceramic bodies composed of anisotropic crystals the stresses resulting from applied loads, large scale residual stresses and localized stresses combine to cause fracture. The localized stresses caused by crystal anisotropy are substantial in magnitude and in large grain size bodies cause local crack formation even in the absence of an applied load. Ceramic bodies of crystals with reduced anisotropy were prepared using compositions in the system Al_2O_3-Cr_2O_3. The variation of strength with grain size was measured and compared with data for alumina bodies. The results were interpreted in terms of variations in grain shape and other microstructural features.

The dimensions of mirrors in fracture surfaces of alumina and alumina strengthened by quenching were measured. Comparison of the flexural stress vs. mirror size curves was used to estimate the residual stresses in the surface of the quenched alumina. The variation of mirror size with temperature was determined. The dimensions of mirrors observed at the axis of quenched specimens that fractured spontaneously were used to estimate the residual stress at the axis. Using this information an experimental residual stress profile was constructed. One exceptional specimen strengthened by quenching had a flexural strength of 223,000 psi.

DD FORM 1 NOV 65 1473 REPLACES DD FORM 1473, 1 JAN 64, WHICH IS OBSOLETE FOR ARMY USE.

I

Security Classification

14. KEY WORDS	LINK A		LINK B		LINK C	
	ROLE	WT	ROLE	WT	ROLE	WT
thermal expansion anisotropy						
elastic anisotropy						
localized stresses						
residual stresses						
alumina						
solid solution						
quenching						
compressive surface layer						
grain size						
grain shape						
flexural strength						
Griffith theory						
fracture mirror						

Ceramic Finishing Company
State College, Pennsylvania

Technical Report No. 6

STRENGTHENING OXIDES BY REDUCTION OF CRYSTAL ANISOTROPY

April, 1972

Prepared by: Henry P. Kirchner
Henry P. Kirchner

Robert M. Gruver
Robert M. Gruver

Prepared under Contract No. N00014-66-C0190 for the Office of Naval Research, Department of the Navy. Requisition Number NR032-498

TABLE OF CONTENTS

III

FOREWORD

This report describes research performed on a program sponsored by the Office of Naval Research, Department of the Navy under Contract N00014-66-C0190. The research was performed under the general technical direction of Dr. Arthur M. Diness of the Office of Naval Research.

The authors are pleased to acknowledge the contributions of their associates at Ceramic Finishing Company including especially Mr. Ralph Walker, Mr. Norman Bierly, Mr. G. William Tasker and Mrs. Ethel Rote. Dr. W. R. Buessem contributed to the program in an advisory capacity.

LIST OF TABLES

V

LIST OF FIGURES

LIST OF FIGURES (Con't)

LIST OF FIGURES (Con't)

I. INTRODUCTION

In single phase polycrystalline ceramic bodies the stresses resulting from applied loads, large scale residual stresses, and localized stresses combine to cause fracture. Localized stresses arise as a result of several phenomena including:

1. Thermal expansion anisotropy
2. Elastic anisotropy
3. Stress concentrations at surface flaws and pores

Presently available evidence indicates that, in strong, well made ceramic bodies, fractures usually originate at flaws ranging in size from about 10 to 300 μm[1-3]. These flaws may be small cracks, large pores, large crystals, etc. Normally, these flaws are located at or near the surface but when the surface flaws are prevented from acting to cause failure by the use of compressive surface layers, fracture may originate in the interior.

The effectiveness of localized stresses in causing fracture seems to depend on the size of the stressed region. Thus, in fine grained bodies localized stresses due to thermal expansion anisotropy have little or no effect on the strength whereas, in coarse grained bodies, these stresses cause localized crack formation and the bodies are weak. The Griffith condition is a necessary condition for fracture to occur and specifies the minimum crack length that can continue to propagate at a given level of stress. It should depend on the combined effect of all types of stresses. However, if the localized stresses act in a region that is very much smaller than the dimensions of a critical flaw or crack, the effect of the localized stresses is presumed to be minimal.

There is considerable uncertainty involved in attempting to describe the mechanisms of fracture of alumina ceramics in various ranges of grain size. Frequently, it has been

assumed that a single mechanism would suffice over the entire range of grain size. However, recent observations of the variations of the relative sizes of the critical flaws and grain size in the various grain size ranges indicate that the mechanism varies with grain size. One approach is to consider the possible influence of the localized stresses in three ranges of grain size.

At grain sizes less than about 2 μm, available evidence[1] indicates that fracture originates at flaws that are much larger than the grain size. In this grain size range, the anisotropy stresses are probably ineffective because they act in a volume that is very small compared with the size of the critical flaws. In the grain size range from about 2 μm to 45 μm, the volume in which the anisotropy stresses act approaches the critical flaw size. In this grain size range, it is reasonable to expect the localized stresses to combine with the stresses due to the applied load to cause failure. The observed decrease in strength, observed in going from 2 μm to 45 μm, is about 40,000 psi[4] and roughly corresponds with estimates of the magnitude of the anisotropy stresses. At grain sizes greater than 45 μm, localized cracks form and the bodies are weak. In this grain size range the strength can be considered to depend on the size of the localized cracks.

The importance of localized stresses in determining the strength of ceramic materials has been investigated by Buessem[5], Buessem and Lange[6], Clarke[7], Hasselman[8] and others. Evidence of the importance of localized stresses includes the observation of localized cracks in alumina[4], titania[9], and beryllia[10], the increase in strength with increasing temperature in beryllia[11] and alumina[1] and the thermal expansion hysteresis of numerous ceramic bodies[5].

The magnitude of the localized stresses caused by thermal expansion anisotropy in BeO was measured by Smith

and Weissman[12] using the x-ray diffraction method. The average stress is 28,000 psi in BeO bodies with randomly oriented grains. The maximum stresses occur when neighboring grains have unfavorable mutual orientations and are much higher.

Since it is evident that strength-anisotropy-grain size relations are of basic importance in attempts to prepare strong ceramic bodies, solid solution compositions with reduced crystal anisotropy are desired. Compositions in the systems Al_2O_3-Cr_2O_3 and TiO_2-VO_2 that are more thermally isotropic than the pure end members were investigated[13]. In the present investigation, polycrystalline ceramic bodies were prepared from some of these compositions in the system Al_2O_3-Cr_2O_3.

Substantial strengthening has been achieved by forming compressive surface layers on polycrystalline ceramic bodies[4,14-16]. Quenching was one of the methods used to form compressive surface layers on alumina, and Al_2O_3-Cr_2O_3 bodies with reduced crystal anisotropy, and improvements in strength were observed.

Another objective is to develop methods of quantitative analysis of fracture surfaces. Substantial progress has been made in the analysis of mirrors formed in the fracture surface of glass specimens. The dimensions of these mirrors are characteristic of the locally acting stresses when fracture occurs. This characteristic has been used to estimate the residual stresses induced by quenching in polycrystalline alumina ceramics.

The procedures used in this investigation are described in the next section. In the section following that the results of the investigation of strengthening by reduction of crystal anisotropy are presented and discussed. In Section IV the results of the analysis of residual stresses based upon the measurement of mirrors in the fracture surfaces of quenched alumina are presented.

II. PROCEDURES

Polycrystalline alumina ceramics and Al_2O_3-Cr_2O_3 solid solution ceramics with reduced crystal anisotropy were prepared by hot pressing. The starting materials were Linde A alumina (0.3 μm grain size, Union Carbide Corp., San Diego, Calif.) and Fisher Certified Cr_2O_3. In some cases MgO was added in the form of magnesium acetate as a grain growth inhibitor. The magnesium acetate was dissolved in methanol, the oxide powders were added, mixed in a Waring blender, dried, and granulated through a 100-mesh sieve. The granulated powder was placed in a graphite die, usually 2-7/8 in. in diameter, and heated in an induction furnace. The time, temperature,* and pressure were varied to obtain billets with various grain sizes.

Cylindrical rods from 0.09 to 0.15 in. in diameter were machined from the billets. The rods were polished using 220, 320, 400 and 600 grit silicon carbide paper and 15 μm diamond paste.

In some cases the polished rods were strengthened by quenching. These rods were heated individually in an induction furnace and then quenched by thrusting the rod into a liquid quenching medium such as silicone oil.

Unless specified otherwise, the flexural strengths of the ceramics were measured by four point loading on a one inch span with rolling contacts, at a stressing rate of about 50,000 psi per minute. The humidity of the test environment was controlled at 20% relative humidity.

The density, porosity, grain size and shape, and other microstructural features of the specimens were studied. The density and porosity were measured by immersion in water. The densities listed in this report are the bulk density (weight per unit volume including both open and closed pores) expressed as a percentage of the theoretical density of the completely non porous composition. The

---

* Temperature measured through top punch.

porosities are reported as the percent porosity due to open pores only. The theoretical density of pure α-alumina is 3.987 gm cm^{-3}. The densities of the solid solution compositions were based upon the results of Rossi and Lawrence[17].

Fracture surfaces, and polished and etched specimens were studied by optical, electron and scanning electron microscopy. The specimens were polished with 6 μm diamond compound on a cast iron lap followed by a tin lap. The polished specimens were chemically etched in concentrated H_2SO_4 for 30 sec. at 300°C; then thermally etched at 1500°C for five minutes.

The average grain size was measured by the circular intercept method described by Hilliard[18]. The reciprocal of the number of intersections per unit length was used directly as the measure of grain size. In other words, no corrections were made for the errors that result because the portions of the grains exposed in the surface of the cross section are smaller on the average than the maximum grain dimension and the circle crosses the grains in a random position.

The mirror diameters were measured using an American Optical microscope with a 40 mm focal length objective (2.6X) and a 25 mm focal length eyepiece (10X). The fracture was observed by using oblique reflected light. A micrometer disc ruled to 0.05 mm was used in the eyepiece to measure the mirror diameter, the distance from the mirror center to the rod axis for internal flaws, and the rod diameter.

For mirrors formed by surface flaw failure, the diameter was measured by taking twice the distance from fracture origin at the edge of the rod to where hackle begins. For internal flaws, the distance from hackle on one side of the fracture origin to hackle on the other side of it was measured as the mirror diameter. In polycrystalline alumina the boundary between the mirror zone and hackle is often much less distinct than in glass but in general it is

the area where flakes and roughness begin.

Electron micrographs of some specimens were prepared by W. W. Corbett, electron microscopist at the Pennsylvania State University, using a Philips E.M. 300 electron microscope. Carbon replica techniques were used to prepare the specimens from fractured, or polished and etched surfaces.

The scanning electron micrographs were prepared by Mrs. Jana Lebiedzik at the Pennsylvania State University using a Japan Electron Optics Laboratory Co. Ltd. Model JSM microscope. The specimens were prepared by evaporating a thin layer of gold on the fractured or polished and etched surface in order to drain off the charge from the electron beam.

X-ray diffraction analyses were performed using a General Electric XRD-5 diffractometer. The x-ray method was used to look for the presence of second phases and to determine the composition of the solid solutions after hot pressing.

III. STRENGTHENING BY REDUCTION OF CRYSTAL ANISOTROPY

A. Effect of Processing Variables and Composition on Grain Size

1. Heating Rate

In the early stages of this research extreme difficulty was encountered in attempts to increase the grain size of the Al_2O_3-Cr_2O_3 bodies. For example, in the most recent report[4], the largest average grain size of the solid solution specimens for which strengths were determined was about 20 μm. In order to achieve this grain size it was necessary to hold the material at 1800°C* for five hours.

In an attempt to obtain increased average grain size, a lower heating rate was used. The temperature was raised to 1000°C in one hour and then to the holding temperature over the following four hours, making a total of five hours to the holding temperature. Previously, the die was raised to the holding temperature as rapidly as possible and usually reached the holding temperature in two or three hours.

This lower heating rate allows more time for densification in the temperature range near 1200°C where rapid densification occurs. Therefore, fewer pores are likely to be trapped in the body. One reason to expect more grain growth with this heating schedule is that fewer pores are likely to be present to inhibit grain growth. Another advantage of the slower heating is that more opportunity is provided for evaporation of adsorbed gases and other impurities at low temperatures before they are trapped. Using the lower heating rate, substantially larger grain sizes were achieved at lower temperatures than were used previously. The maximum average grain size was 57 μm which resulted from holding at 1650°C for five hours.

---

* Temperature measured on the outside of the die body. For comparison with the present measurements subtract about 100°C.

2. Pressing Temperature and Time

When the Al_2O_3-Cr_2O_3 solid solution bodies are made by hot pressing mixtures of pure oxide powders, the minimum temperature and pressing time are determined by the need to obtain complete reaction of the oxides. X-ray diffraction analysis of a body pressed at 1325°C for one hour showed that the reaction was not quite complete. With this heat treatment the diffraction peaks of the starting powders had disappeared but those of the solid solution were broader than they should be for a homogeneous solid solution. After pressing at 1325°C or 1350°C for two hours the diffraction peaks were considerably less broad.

At the highest hot pressing temperatures some problems were encountered. One of these problems was loss of material from the die cavity. For example, a 72% Al_2O_3-28% Cr_2O_3 billet, hot pressed at 1650°C for five hours, showed a weight loss of 27%. For comparison, a similar billet pressed at 1500°C for two hours had a weight loss of 2%.

Several possible mechanisms of weight loss were considered. Among these mechanisms were:

1. Evaporation of chromium oxide.
2. Extrusion of material from the die cavity.
3. Reduction to form lower oxides.

X-ray diffraction analysis was used to determine the phases present and the composition of the Al_2O_3-Cr_2O_3 solid solution. The diffraction patterns showed that only one phase was present and that phase was the Al_2O_3-Cr_2O_3 solid solution. The composition was determined based upon the location of the 146 diffraction peak located at about 133°2θ. The results of these analyses are presented in Table I. They show that there is a substantial reduction in the chromium content of the solid solution but this reduction is not sufficient to account for the 27% weight

TABLE I

Analysis of Al_2O_3-Cr_2O_3 Solid Solution Compositions

Description of Specimen				
Billet No.	Pressing Temp. °C	Hold Period Hours	Location of 146 Peak Degrees 2θ	Composition % Cr_2O_3
8-55-1	1325	2	132.46	28.7
8-63-3 (0.25% MgO)	1350	2	132.7	26.5
8-89-1	1650	5	133.06	23.3
8-89-1	1650	5	133.12	22.8
8-89-3 (0.25% MgO)	1650	5	133.1	22.9
Al_2O_3 powder			136.11	none

loss of the billet.

The densities of some of these billets were determined. The results are presented in Table II. The densities of the billets pressed at low temperatures were greater than 99.6% of theoretical density. Based upon the assumption that the solid solution composition of the specimens pressed at 1650°C was 28% Cr_2O_3 the densities of specimens seem lower than should be expected. However, when the average solid solution composition, 23% Cr_2O_3, from Table I" is used to calculate the percent of theoretical density, the values range from 99.3 to 99.9 percent which seems much more reasonable. Therefore, based upon both x-ray analysis and density determinations, it is evident that the Cr_2O_3 content of the solid solutions pressed at 1650°C has been reduced and the actual composition is approximately 77% Al_2O_3-23% Cr_2O_3.

Examination of the die wall of the die used to press the billets at 1650°C revealed the presence of material not usually observed there after pressing at lower temperatures. This material has not been characterized but it appears to have been extruded or squeezed from the die cavity. Therefore, it is concluded that most of the material that was lost from the die was lost by this extrusion process. The change in composition from 28% Cr_2O_3 to 23% Cr_2O_3 represents a weight loss of 7 to 8% assuming that only Cr_2O_3 was lost by evaporation. Apparently the balance of the loss, 19-20%, was lost by extrusion from the die cavity.

The x-ray diffraction patterns of the billets that were hot pressed at 1650°C showed some other features that should be noted. In patterns taken from surfaces cut parallel to the pressing direction the intensity of some peaks is lower than would be expected based upon examinations of specimens pressed at lower temperatures or specimens that were pressed at the same temperature that were powdered before x-ray

TABLE II

Density of Hot Pressed Billets
of Al_2O_3-Cr_2O_3 Solid Solution

Billet No.	Pressing Temp. °C	Hold Period Hours	Density gm cm^{-3}	Percent of Theoretical Density Based on 28% Cr_2O_3	Based on 23% Cr_2O_3
8-55-1	1325	2	4.35	99.7	---
8-63-3 (0.25% MgO)	1350	2	4.34	99.6	---
8-93-1	1500	2	4.34	99.6	---
8-89-1	1650	5	4.25	97.6	99.3
8-89-2 (0.1% MgO)	1650	5	4.29	98.4	99.8
8-89-3 (0.25% MgO)	1650	5	4.28	98.1	99.6

examination. Therefore, there seems to be a substantial degree of preferred orientation in this material. This observation is unexpected based upon the rounded nature of the grains as indicated later.

Some of the diffraction peaks at higher angles are rather broad, perhaps indicating that the solid solutions pressed at high temperature have a tendency to decompose. Some of the photomicrographs presented in later sections of this report have a checkered substructure which may be further evidence of decomposition.

3. Effect of Magnesia Additions

Magnesia is effective as a grain growth inhibitor in Al_2O_3-Cr_2O_3 solid solution ceramics as well as in alumina bodies. The effect of various magnesia additions on the average grain size of the 72% Al_2O_3-28% Cr_2O_3 solid solution composition is shown in Figure 1. The scattered data points at 0.05 and 0.10% MgO for the specimens pressed at 1650°C may be the result of temperature variations in the die. Nevertheless, the trend of grain size with composition is evident.

The microstructures of the two series of specimens are presented in Figures 2-5. The decrease in average grain size with increasing MgO content is clearly illustrated. In addition, there is an increasing occurrence of black spots on grain boundaries and at triple points with increasing MgO content. These black spots are pores or pullouts as shown in Figure 5.

None of these microstructures show the typical variations in grain size and grain shape expected in strong bodies. The microstructures in Figure 2 (1525°C) show angular, elongated grains with a wide range of grain sizes. The microstructures in Figure 4 (1650°C) show rounded grains with a wide range of grain sizes and a bimodal grain size distribution. Further comments on these microstructures will be made in the next section.

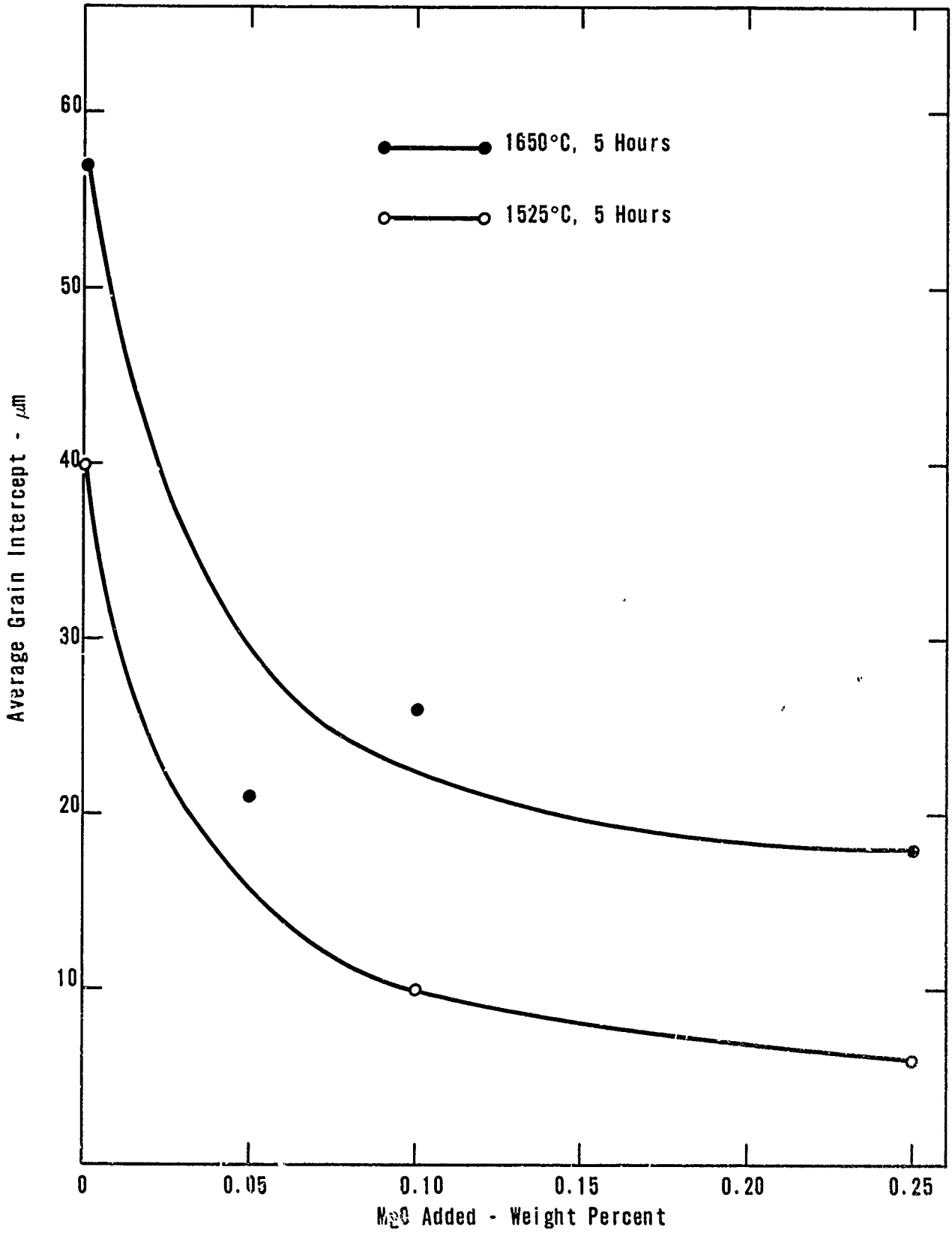

Figure 1 Effect of Magnesia Additions on the Grain Size of 72% Al_2O_3-28% Cr_2O_3 Solid Solution

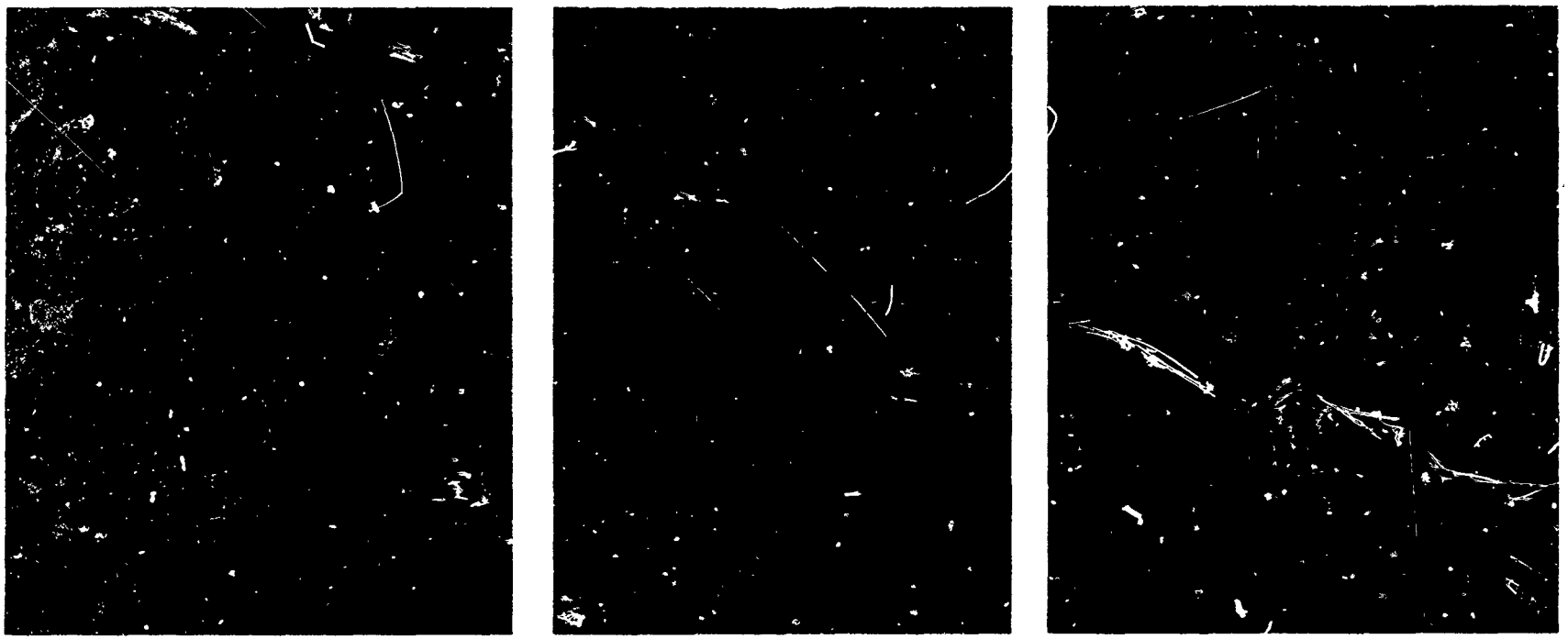

A. 0% MgO

B. 0.1% MgO

C. 0.25% MgO

10μm

Figure 2 72% Al_2O_3-28% Cr_2O_3 Specimens with Various Additions of MgO, Hot Pressed at 1525°C for 2 Hours (290X)

1 μm

Figure 3 72% Al_2O_3-28% Cr_2O_3 Specimen with 0.25% MgO added, Pressed at 1525°C for 2 Hours (2620X) Same as Figure 2C.

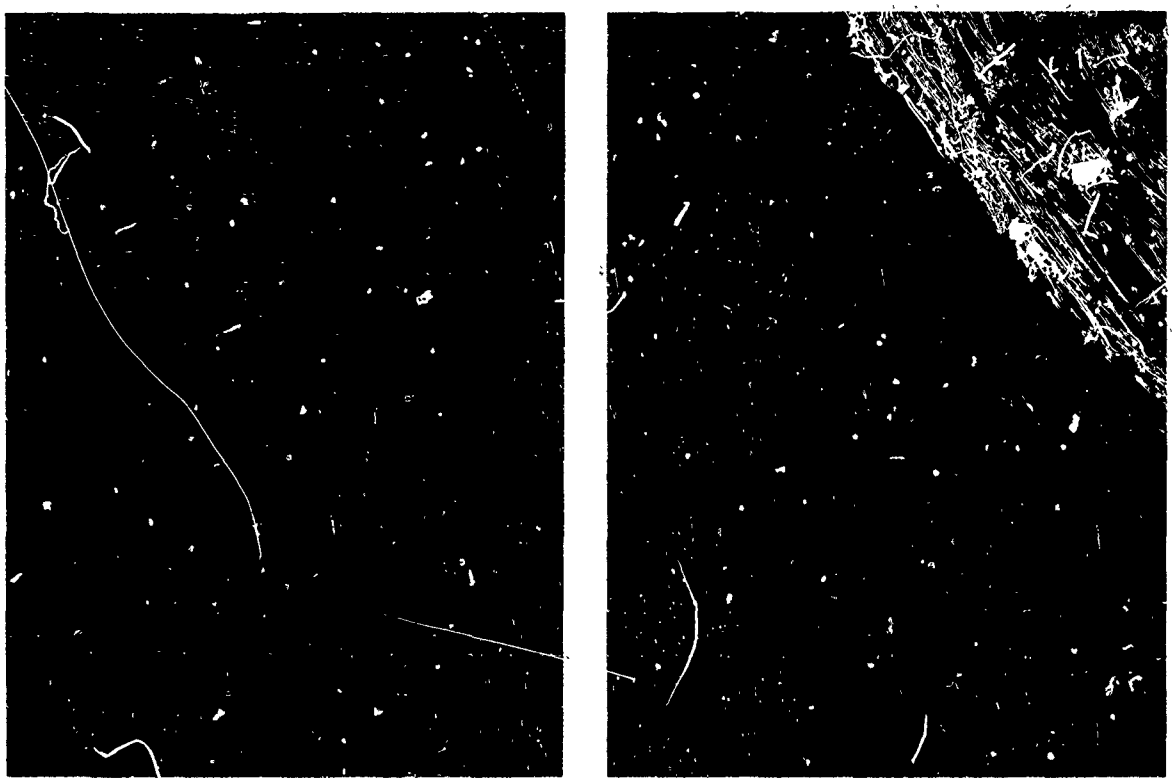

A. 0% MgO

100 μm

B. 0.05% MgO

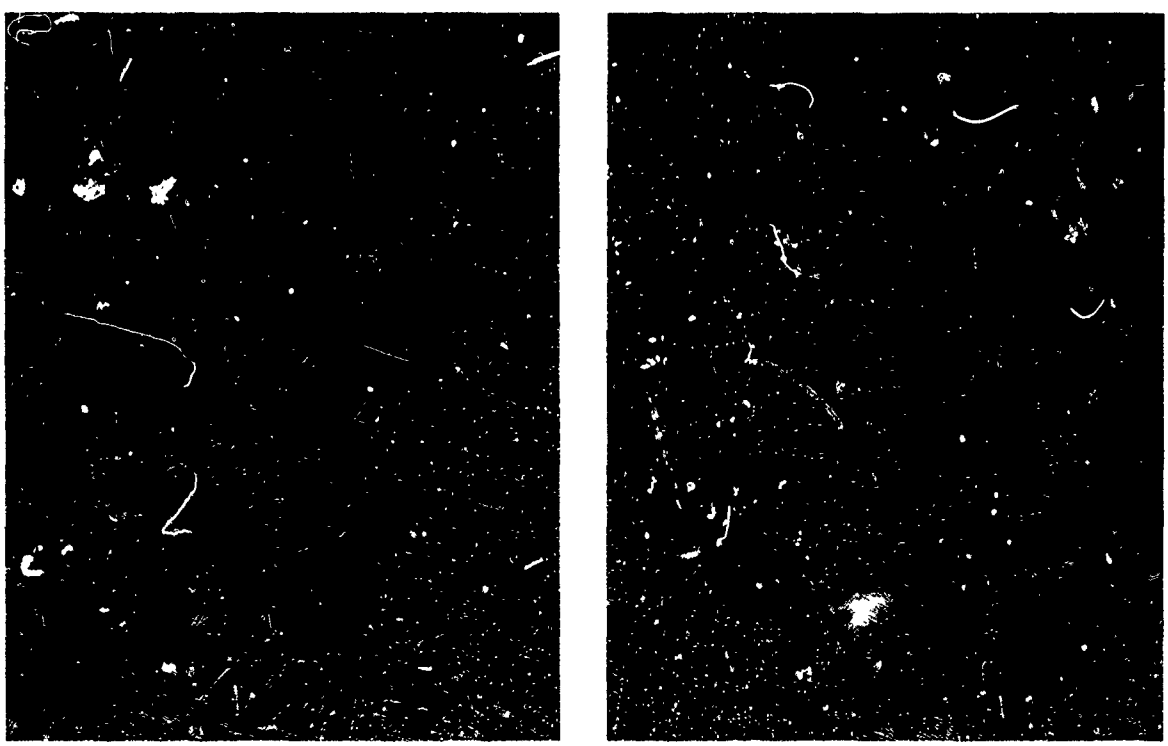

C. 0.1% MgO

D. 0.25% MgO

Figure 4 72% Al_2O_3-28% Cr_2O_3 Specimens with Various Additions of MgO, Hot Pressed at 1650°C for 5 Hours (110X)

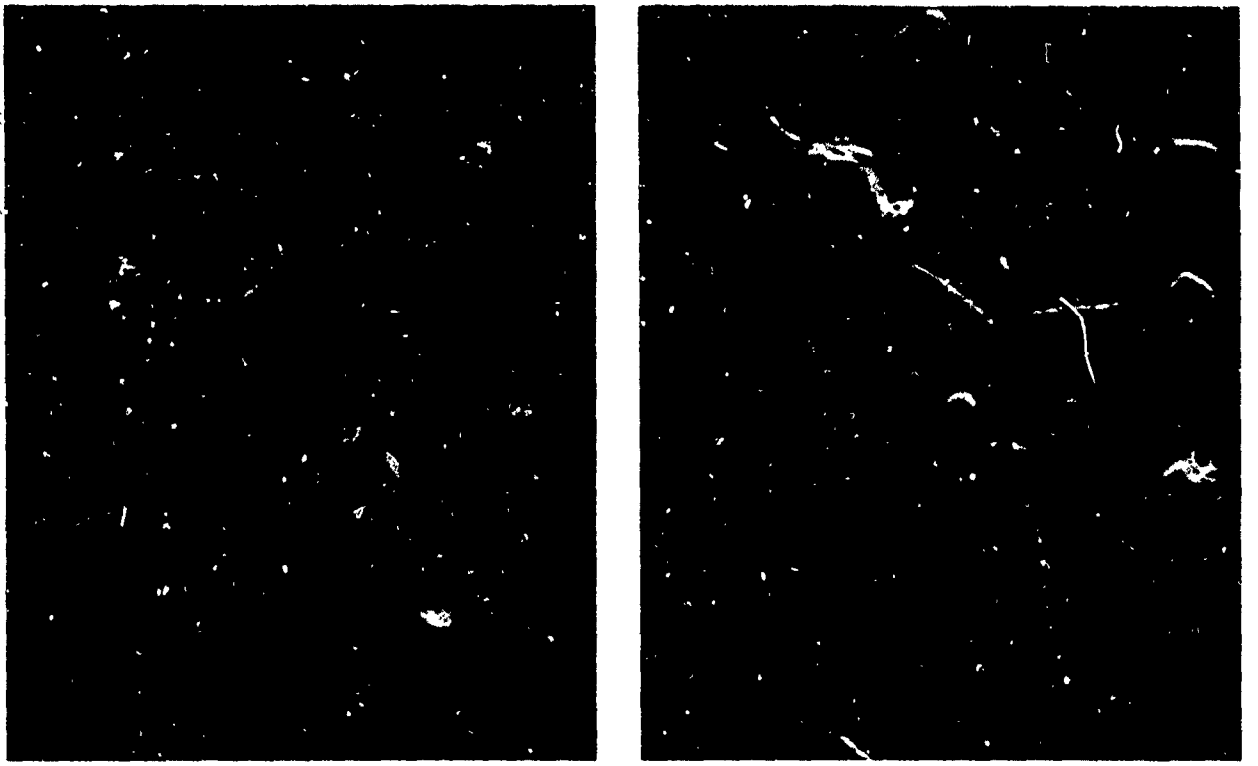

A. 0% MgO

10μm

B. 0.25% MgO

Figure 5 Scanning Electron Micrographs, 72% Al_2O_3-28% Cr_2O_3 Specimens Hot Pressed at 1650°C for 5 Hours (1000X)

B. Effect of Processing Variables and Composition on Grain Shape

1. Pressing Temperature and Time

It has been known for some time that alumina tends to form lathlike grains as higher sintering temperatures are used. This feature was well illustrated for sintered alumina by Cahoon and Christenson[19]. Similar lathlike grain growth was illustrated for alumina hot pressed at 1625°C for four hours to form a 30 μm body[4]. Additions of magnesia are very effective in inhibiting grain growth in alumina bodies. Even after hot pressing at high temperatures for long periods of time the average grain size is limited to less than 10 μm. In alumina bodies with magnesia additions that are sintered to full density at high temperatures (for example, LUCALOX) the lathlike grain growth is avoided[20].

The 72% Al_2O_3-28% Cr_2O_3 composition tends to form somewhat elongated (approximately 2:1 or 3:1 length to width ratio) grains in bodies with a two micrometer average grain size obtained by hot pressing at 1480°C* for one hour. The microstructure of this body was illustrated in a previous report[21]. When this composition was pressed at higher temperatures such as 1700-1800°C* to form a body with an average grain size of 20 μm, the lathlike structure became more pronounced.

Additional evidence of this tendency to form elongated grains has been obtained for bodies with both smaller and larger grain sizes. Figure 6 shows elongated grains in a body with an average grain size of 0.85 μm obtained by heating according to the slower schedule and pressing at

* measured on the outside of the die

Figure 6 72% Al_2O_3-28% Cr_2O_3 Body, 0.85 μm Grain Size, Hot Pressed at 1375°C for 2 Hours (26,000X)

1375°C for two hours. The larger grain size body was obtained by pressing at 1525°C for two hours and has an average grain size of 40 μm. The microstructure of this body is shown in Figure 7.

The elongated microstructures observed in these bodies bear some resemblance to the lathlike microstructures observed in pure alumina bodies when the grains begin to grow. Cahoon and Christenson[19] state that additions of Cr_2O_3 to sintered alumina in amounts above one weight percent alter the shape to nearly spheroidal and that additions over 7% cause the grains to be increasingly more equiaxed and ragged in appearance. The present observations for this 27 mole percent composition formed by hot pressing seem to have much different microstructures from those described by Cahoon and Christenson.

In one series of specimens more nearly spheroidal grains were observed, especially in the compositions containing magnesia additions, as shown in Figure 4. Since the maximum grain size of the specimens with magnesia additions is well over twice the average grain size, the microstructures are typical of abnormal or discontinuous grain growth as described by Hillert[22]. The microstructures shown in Figure 2 have very lathlike grains and span much of the same grain size range as those in Figure 4. No explanation is available, at present, for the wide variations in grain shape observed for specimens of approximately equivalent grain size.

2. Prereacted powders

In the early stages of this research, the powders used for hot pressing were either (1) mixtures of the oxide powders or (2) coprecipitated hydroxides. In both cases lathlike crystals were formed when the pressing was carried out at high temperatures and for long times in order to grow large grains.

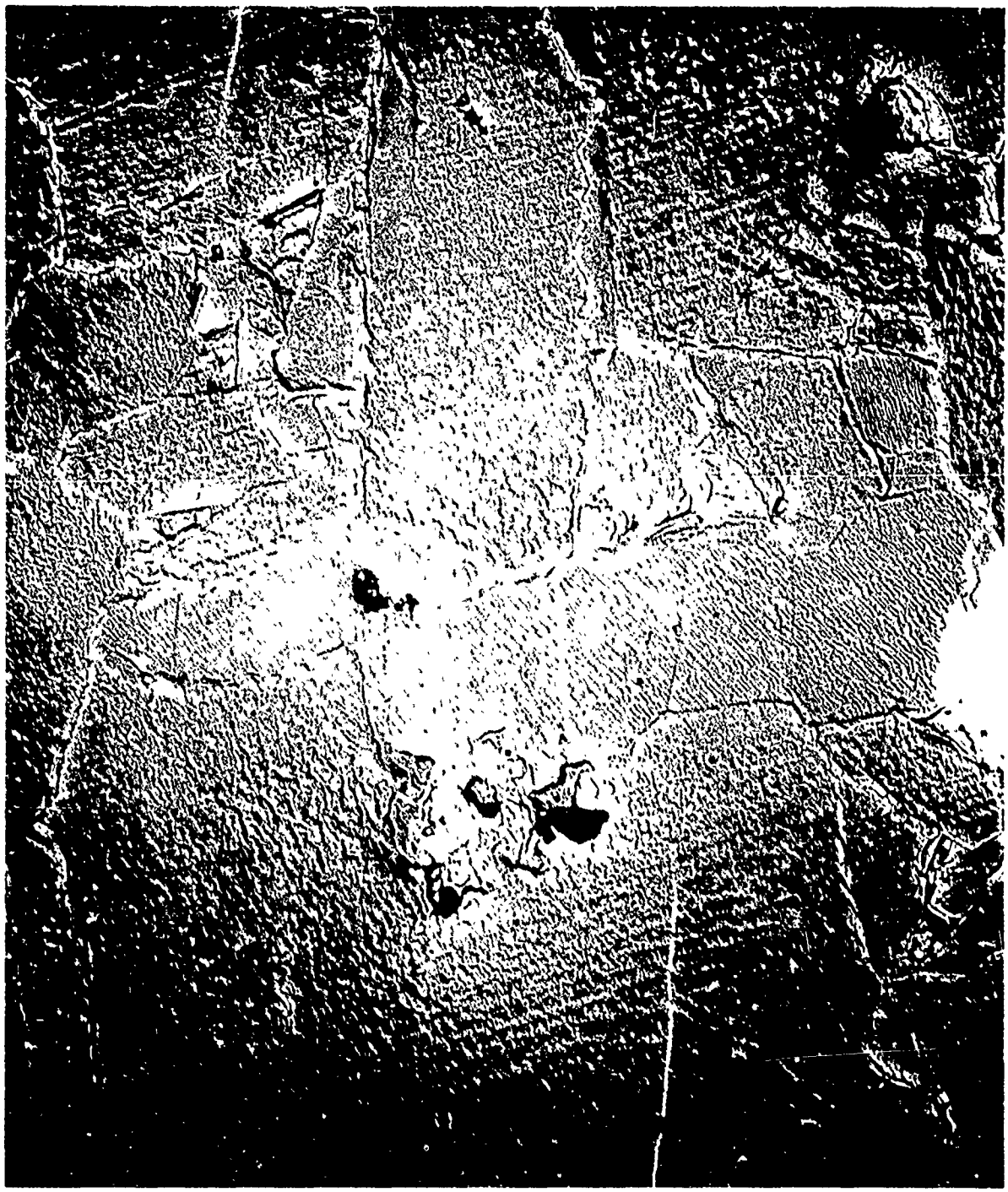

Figure 7 72% Al_2O_3-28% Cr_2O_3 Body, 40 μm Grain Size, Hot Pressed at 1525°C for 2 Hours (2130X)

One attempt at preventing the occurence of lathlike grains involved the use of prereacted powders. The oxide powders were mixed and then reacted by firing at 1400°C for four hours. This temperature is high enough so that reaction of the powders can be assumed to be essentially complete. The resulting material was ball milled for two hours in methanol to reduce the particle size.

Billets of the solid solution were hot pressed from both mixed oxide powders and prereacted powders. The materials were hot pressed at 1800°C (measured on the outside of the die body) at 4000 psi. The resulting billets were characterized. The results are summarized in Table III and the microstructures are compared in Figure 8. The photomicrographs show that similar grain sizes were obtained in both cases and that both microstructures contain similar lathlike crystals. Therefore, this approach to preventing the formation of the lathlike grains was unsuccessful.

C. Strength vs. Composition

Since the effect on the strength of reduction of the thermal expansion anisotropy was expected to be most evident at large grain size, billets of various Al_2O_3-Cr_2O_3 compositions were pressed under conditions (1500°C, 2 hours) expected to yield substantial grain growth. Cylindrical rods were machined from these billets and the flexural strengths were measured. Polished and etched specimens were examined and the average grain size was measured. The microstructures consisted mainly of lathlike grains as shown in Figure 9. The average grain size of the various compositions ranged from 30 to 49 μm. The flexural strengths are given in Figure 10. The observed strengths were relatively low, even compared with the strength vs. grain size curve for the 72% Al_2O_3-28% Cr_2O_3 composition. There

TABLE III

Comparison of 72% Al_2O_3-28% Cr_2O_3 Solid Solution Bodies
Hot Pressed from Mixed Oxidesand Prereacted Powders

	Pressing No. 7-86	Pressing No. 7-132
Powder Preparation		
Type of powder	Mixed oxides (unreacted)	Prereacted
Reaction conditions	---	1400°C, 4 hours
Subsequent processing	---	Ball milled 2 hours in methanol
Hot Pressing Conditions	1800°C*, 5 hrs., 4000 psi	1800°C*, 3-1/2 hrs., 4000 psi
Characterization		
Bulk density, % of theoretical	100	99.3
Open pore porosity, %	0.03	0.01
Average grain size, μm	20	27

* 1800°C measured on the outer surface of the die is equal to approximately 1700°C in the interior.

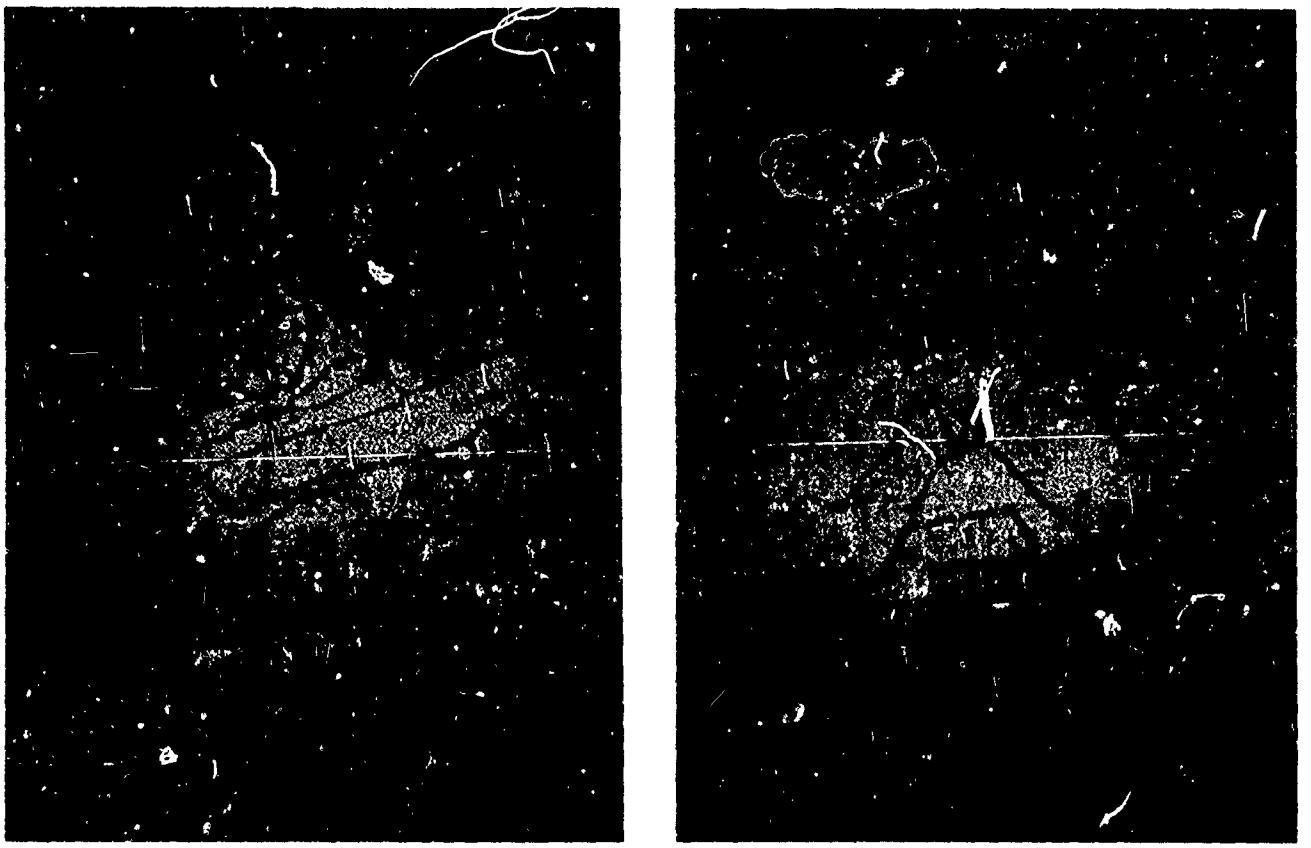

A. Reacted during Hot Pressing

B. Prereacted before Hot Pressing

10 μm

Figure 8 Microstructure of 72% Al_2O_3-28% Cr_2O_3 Solid Solution Bodies made from mixed oxides and Prereacted Powders (430X)

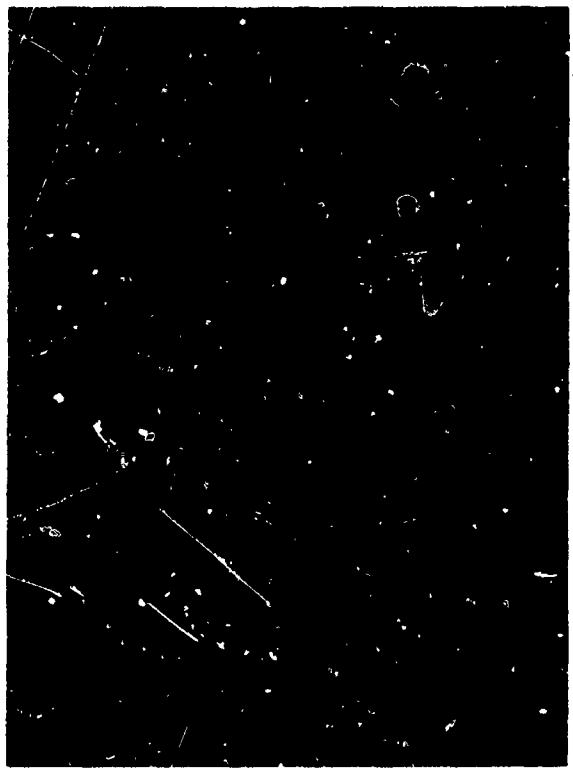

7% Cr_2O_3

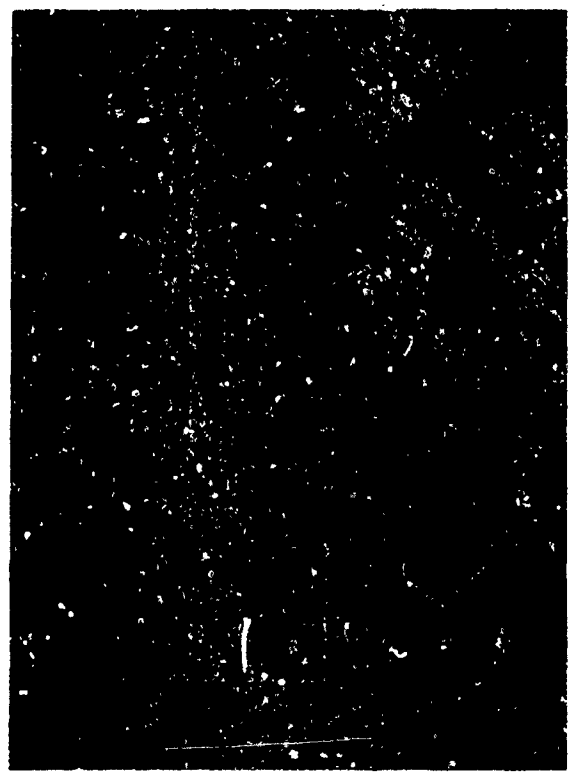

14% Cr_2O_3

21% Cr_2O_3

28% Cr_2O_3

Figure 9 Microstructures of Specimens with Various Compositions in the System Al_2O_3-Cr_2O_3 (110X)

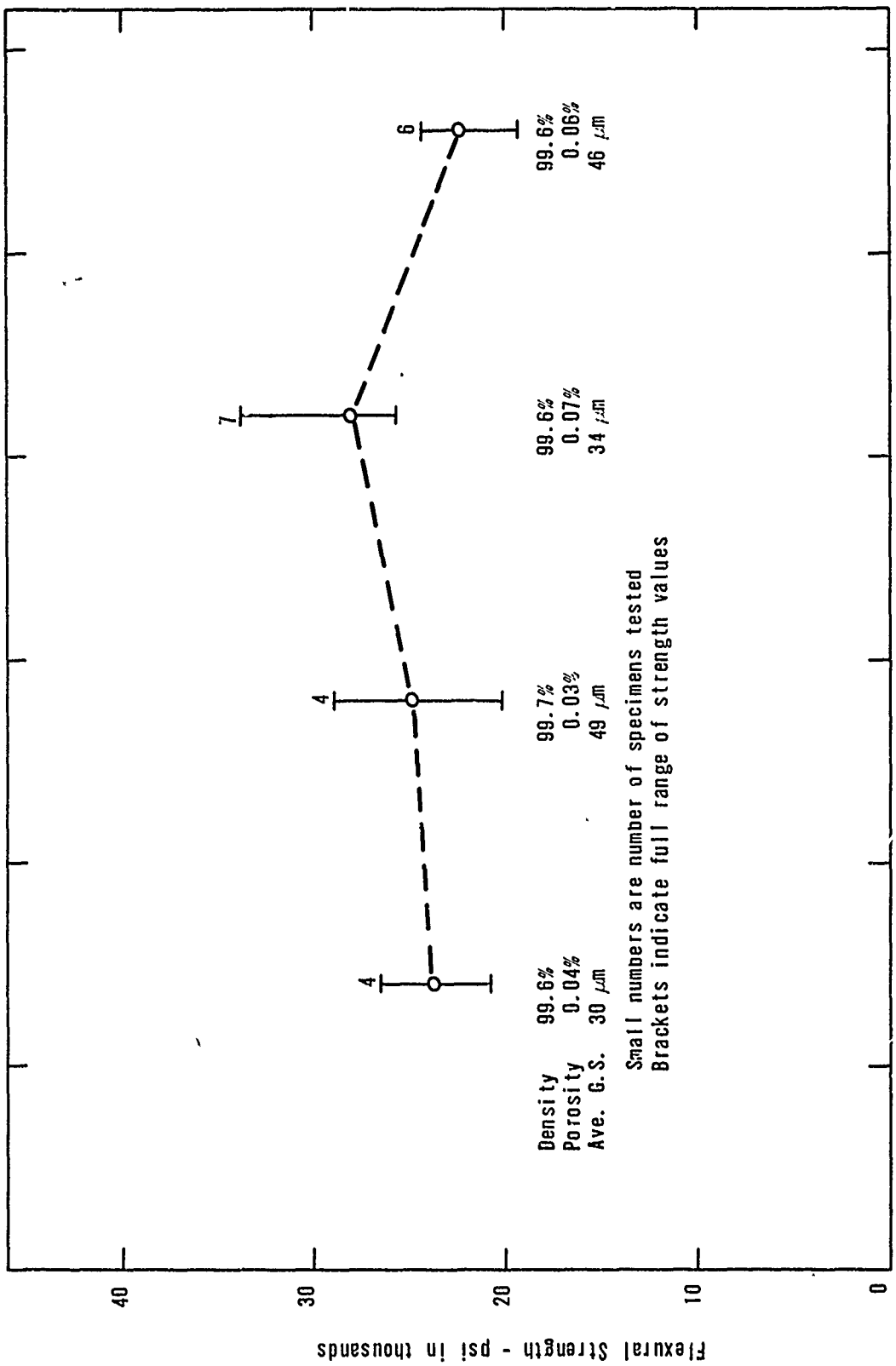

Figure 10 Flexural Strength vs. Composition for Coarse Grained Al_2O_3-Cr_2O_3 Solid Solutions (Pressing No. 8-93, 1500°C, 2 Hours)

was no straightforward variation of strength with grain size. The highest average strength was observed at 21% Cr_2O_3. The results indicate that these observed strengths depend mainly on the grain size and the presence of the lathlike grains rather than the composition or other factors.

D. Strength vs. Grain Size

1. 72% Al_2O_3-28% Cr_2O_3

As described previously, billets of the 72% Al_2O_3-28% Cr_2O_3 composition with reduced crystal anisotropy were hot pressed at various temperatures for various periods of time to obtain bodies with a wide range of average grain sizes. These billets were hot pressed using the slower heating schedule so that larger grain sizes were achieved compared with those resulting from earlier experiments.

Cylindrical rods were machined from these billets and polished. The flexural strengths were measured by four point loading on a one inch span. The results of these measurements are presented in Table IV and Figure 11. At grain sizes less than 0.90 μm, some of the specimens are less dense and the bonds between grains are less strong than desired, so the strength does not continue to increase with decreasing grain size. At grain sizes greater than 0.90 μm the strength decreases with increasing grain size, as expected. The slope of the curve is approximately -0.28, substantially less than the slope of -0.5 that would be expected based on the Griffith theory assuming the flaw size is equal to the grain size.

A type of defect not previously observed in these solid solution specimens was found in some of these bodies. The defect is illustrated in Figure 12. It appears to be a region of unbonded grains in an interstice formed by several large grains. The unbonded grains range in size from about one to ten micrometers so that they are too large to be the

TABLE IV

Flexural Strength of 72% Al_2O_3-28% Cr_2O_3 Composition
(Pressed at 4000 psi, after 5 hour heating schedule except as noted)

	Pressing Conditions		Body Characteristics			
Billet No.	Temp. °C(1)	Hold Period Hours	Density % of theor.	Porosity %	Average Grain Intercept μm	Average Flexural Strength psi
8-46-1	1525	2	99.5	0.15	50	28,000
8-47-1	1475	2	99.6	0.07	30	30,600
8-49-1	1425	2	100.2	0.06	10	46,700
8-52-1	1375	2	99.6	0.11	0.85	74,200
8-55-1	1325	2	99.7	0.12	0.40	88,200
8-60-1	1300	2	98.7	0.20	0.35	78,700
8-61-1(2)	1300	4	99.4	0.20	1.0	73,100
8-63-1	1350	2	99.8	0.05	0.90	88,000
8-65-1(3)	1325	1	99.5	none	0.60	73,300
8-86-1	1600	5	98.2	0.63	44	26,100
8-89-1	1650	5	97.6	0.34	57	17,000
8-93	1500	2	99.6	0.06	46	22,000

(1) center of die (2) 9 hour heating schedule (3) 6000 psi

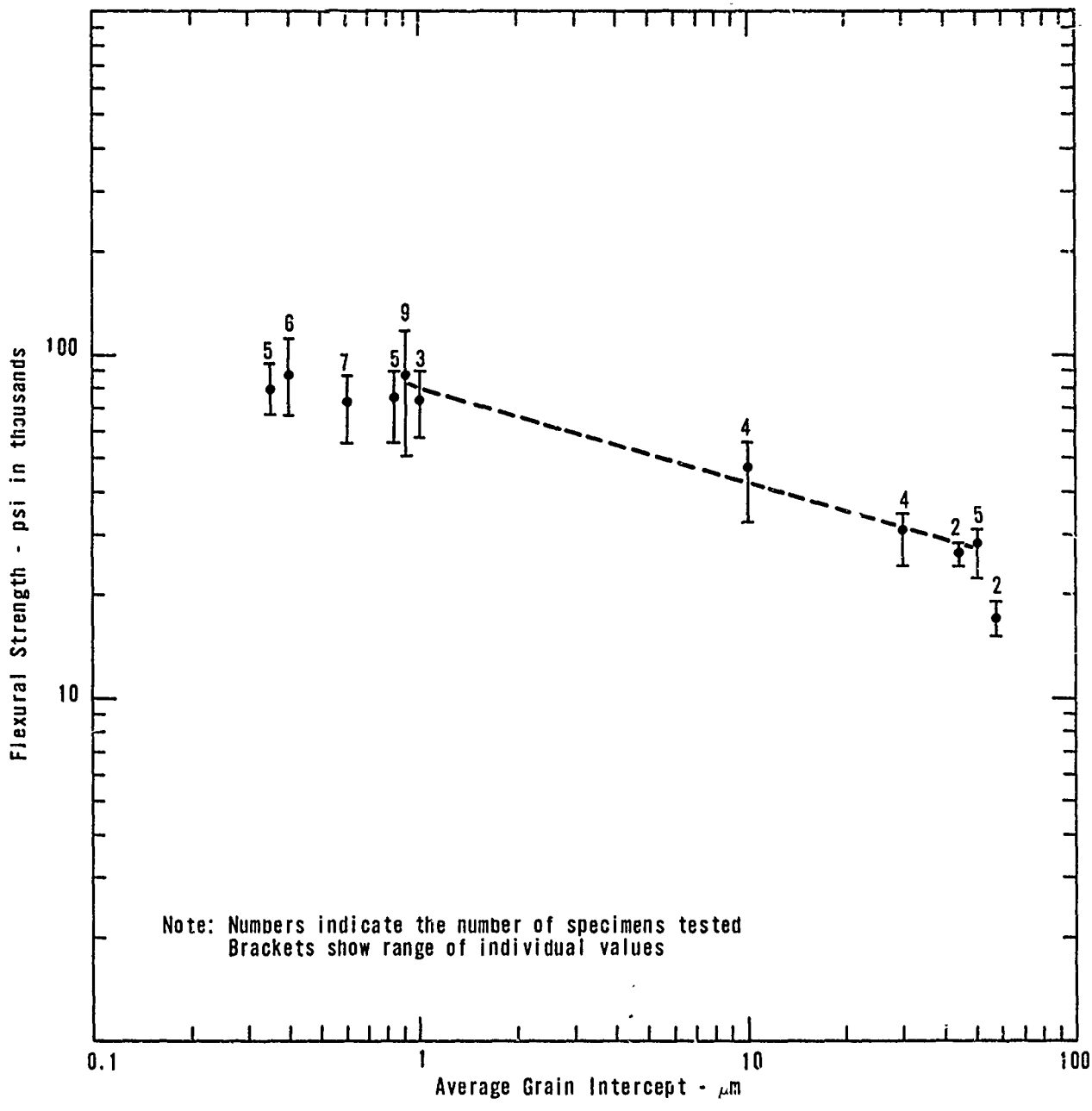

Figure 11 Flexural Strength vs. Grain Size of 72% Al_2O_3-28% Cr_2O_3, No MgO Added

A. 300X

10 μm

B. 3000X

1 μm

Figure 12 Region of unbonded grains in 72% Al_2O_3-28% Cr_2O_3 Body, Billet 8-46-1

original particles. Apparently, at some stage of crystal growth the lathlike growth occurred and these regions did not participate in this growth.

2. 72% Al_2O_3-28% Cr_2O_3 with 0.1% MgO

Magnesia was added as a grain growth inhibitor as described in previous sections. The strength vs. grain size is presented in Table V and Figure 13. The strength remains relatively high, up to an average grain size of about 10μm, and then decreases sharply. No explanation of this decrease is available.

3. 72% Al_2O_3-28% Cr_2O_3 with 0.25% MgO

The strength vs. grain size data for 72% Al_2O_3-28% Cr_2O_3 bodies with 0.25% MgO added as a grain growth inhibitor are presented in Table VI and Figure 14. Based upon these limited data, tnere is little evidence of variation of strength with grain size up to 9.4μm and there is a sharp decrease in strength with grain size at larger grain size. This strength decrease which was noted for the specimens with 0.1% MgO seems more pronounced at 0.25% MgO addition.

4. Comparison of Strength vs. Grain Size Results

The strength vs. grain size results for various magnesia additions and heating rates are compared in Figure 15. This comparison shows that the earlier data[8,21] based on the faster heating schedule yielded the strongest specimens. The slower heating schedule is useful mainly to remove pores and allow the preparation of coarse grained bodies. The specimens with the magnesia additions are comparatively strong at about ten micrometer grain size and relatively weak at larger and smaller grain sizes.

Literature data of Spriggs and Vasilos[23] for pure alumina corrected to zero porosity are included in the figure for comparison. The 72% Al_2O_3-28% Cr_2O_3 bodies have

TABLE V

Flexural Strength of 72% Al_2O_3-28% Cr_2O_3 Composition with Addition of 0.1% MgO

(Pressed at 4000 psi after 5 hour heating schedule)

Billet No.	Pressing Conditions: Temp. °C(1)	Pressing Conditions: Hold Period Hours	Body Characteristics: Density % of theor.	Body Characteristics: Porosity %	Average Grain Intercept μm	Average Flexural Strength psi
8-46-2	1525	2	99.8	0.03	10	60,100
8-47-2	1475	2	99.6	0.07	5.2	71,000
8-49-2	1425	2	99.7	0.02	2.3	77,300
8-86-2	1600	5	100.6	0.10	14	42,200
8-89-2	1650	5	98.4	0.31	26	26,000

(1) Temperature measured in center of die

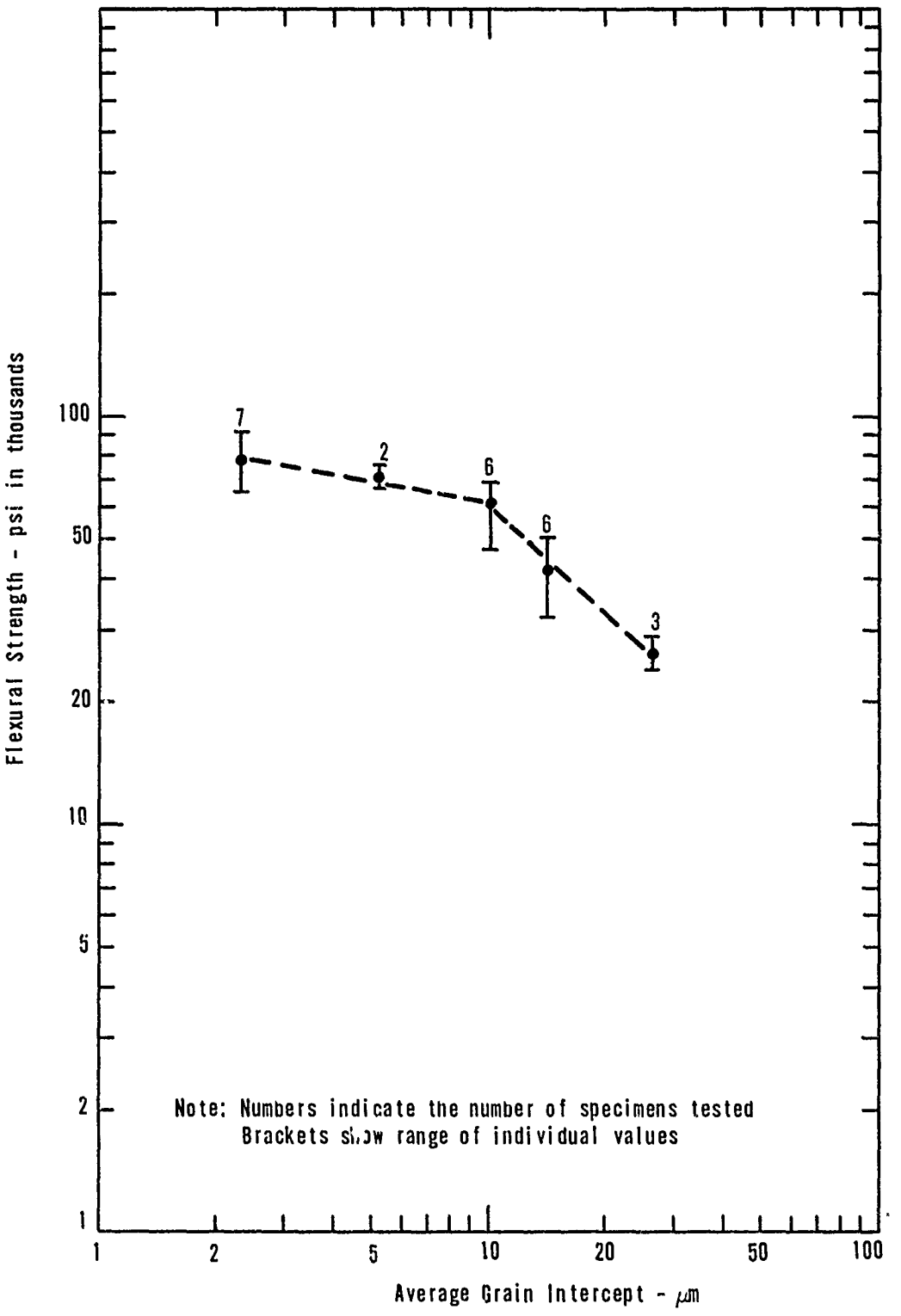

Figure 13 Flexural Strength vs. Grain Size of 72% Al_2O_3-28% Cr_2O_3, 0.1% MgO Added

TABLE VI

Flexural Strength of 72% Al_2O_3-28% Cr_2O_3 Composition
with Addition of 0.25% MgO
(Pressed at 4000 psi, after a 5 hour heating schedule)

	Pressing Conditions		Body Characteristics			
Billet No.	Temp. °C.(1)	Hold Period Hours	Density % of theor.	Porosity %	Average Grain Intercept μm	Average Flexural Strength psi
8-46-3	1525	2	99.6	0.04	9.4	69,800
8-47-3	1475	2	99.5	0.16	4.5	66,900
8-49-3	1425	2	100.4	0.10	2.5	71,300
8-86-3	1600	5	99.4	none	11	49,800
8-89-3	1650	5	98.1	0.30	18	24,100

(1) Temperature measured in center of die

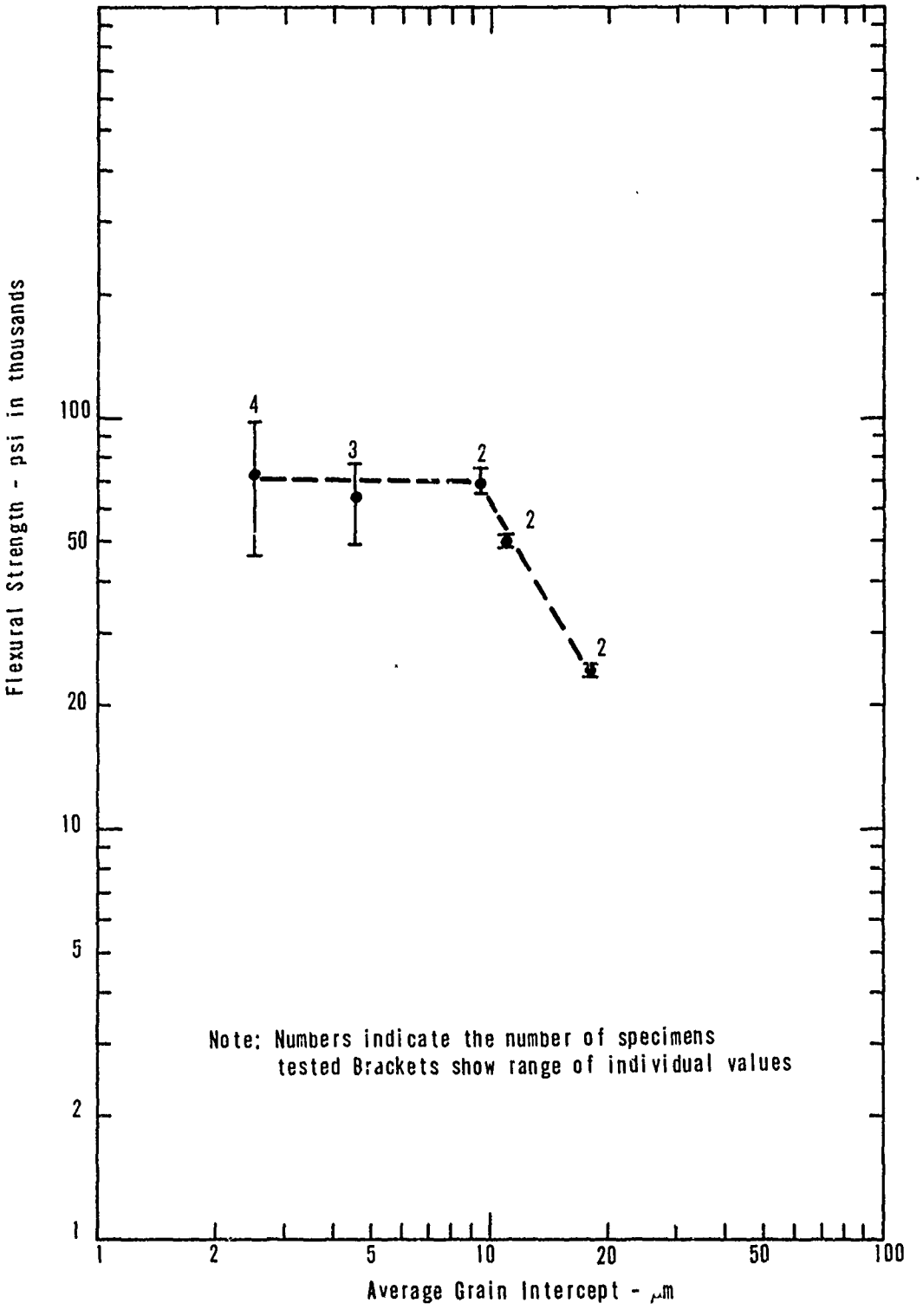

Figure 14 Flexural Strength vs. Grain Size of 72% Al_2O_3-28% Cr_2O_3, 0.25% MgO Added

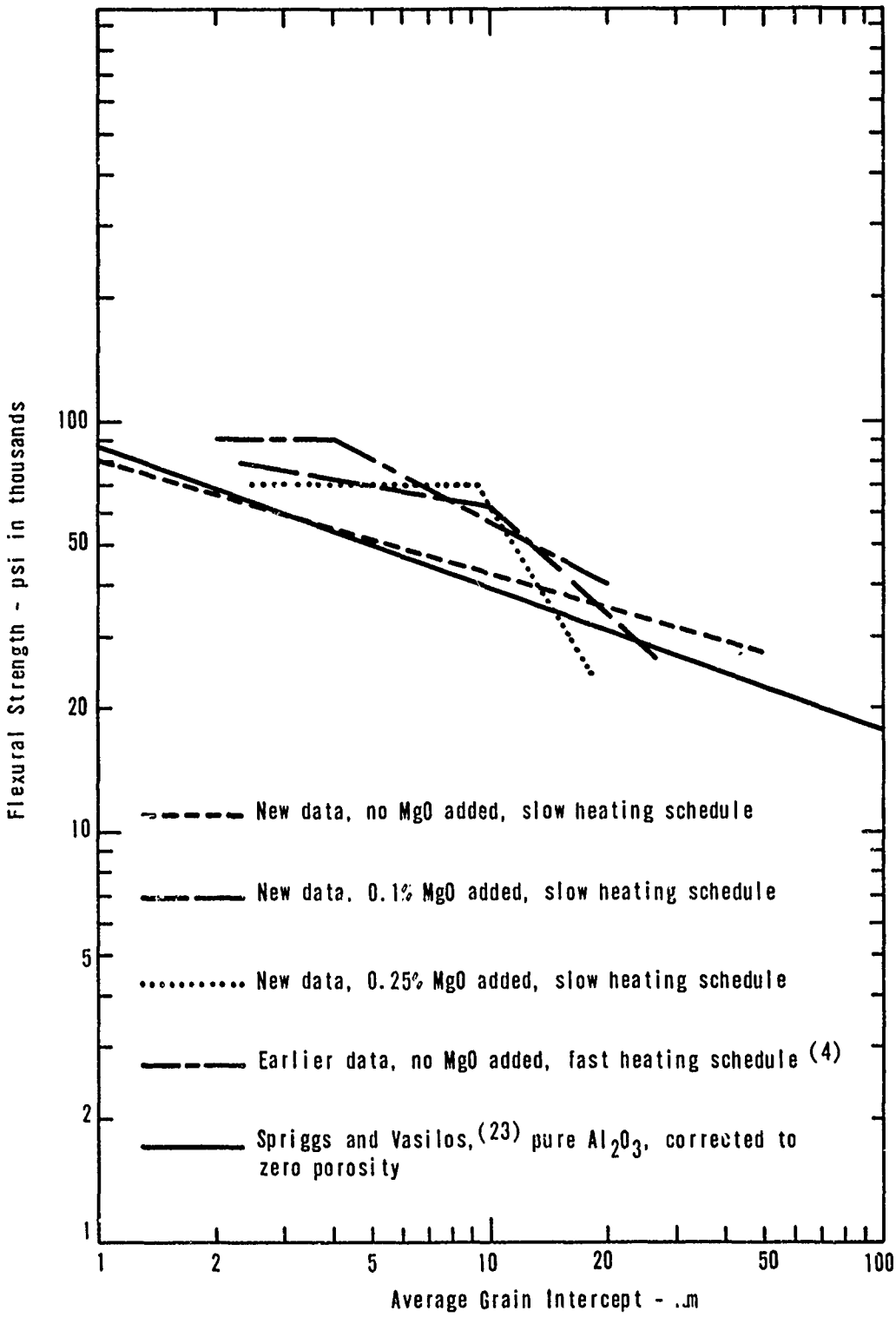

Figure 15 Comparison of Flexural Strength vs. Grain Size for Various Magnesia Additions and Heating Rates

higher measured strengths than this alumina especially in the intermediate grain size range. These differences may be greater than indicated on the figure because of the different methods of measuring grain size. The Spriggs and Vasilos measurements of grain size are the average of the diameters of ten grains taken at random. This method probably tends to give higher average grain sizes because the largest distance from grain boundary to grain boundary is used rather than the length of the random path obtained by the circular intercept method. If this is correct the Spriggs and Vasilos data should be moved to the left an unknown amount.

Other data for the strength vs. grain size of alumina are available for hot pressed alumina[4] made at Ceramic Finishing Company and sintered alumina[24] (LUCALOX) from General Electric. The flexural strengths of these specimens are approximately equal to the average strengths of the best groups of 72% Al_2O_3-28% Cr_2O_3 specimens. Thus, it is not certain that the improved strength expected as a result of reduction of crystal anisotropy has been demonstrated.

The flexural strengths of individual specimens in selected groups of specimens are given in Table VII. These results provide ample evidence that good strengths can be achieved in these compositions, at least at fine grain size. The fracture surface of the specimen with a flexural strength of 118,400 psi is shown in Figure 16. This fracture is similar to those usually observed for alumina bodies at this strength level. The fracture surface shows the fracture origin at the top of the picture surrounded by the "mirror". Radiating ridges and valleys (hackle) are present and are quite pronounced as expected in fractures at relatively high stresses.

It was anticipated that the advantages of reduced crystal anisotropy would be most evident at large grain size. Relative

TABLE VII

Flexural Strength of Selected Groups of Specimens

Composition	72% Al_2O_3-28% Cr_2O_3		72% Al_2O_3-28% Cr_2O_3 + 0.1% MgO		72% Al_2O_3-28% Cr_2O_3 + 0.25% MgO
Billet No.	8-63-1	8-55-1	8-52-2	8-55-2	8-49-3
Specimen No.					
1	118,400	110,700	94,700	106,800	96,200
2	108,200	103,200	89,100	75,000	94,900
3	99,900	95,800	87,300	74,100	47,100
4	99,100	79,600	82,100	64,480	46,500
5	86,700	74,100	61,800	62,700	--
6	83,700	66,000	--	54,200	--
7	82,100	--	--	49,000	--
8	63,100	--	--	--	--
9	50,800	--	--	--	--
Average	88,000	88,200	83,000	69,500	71,300

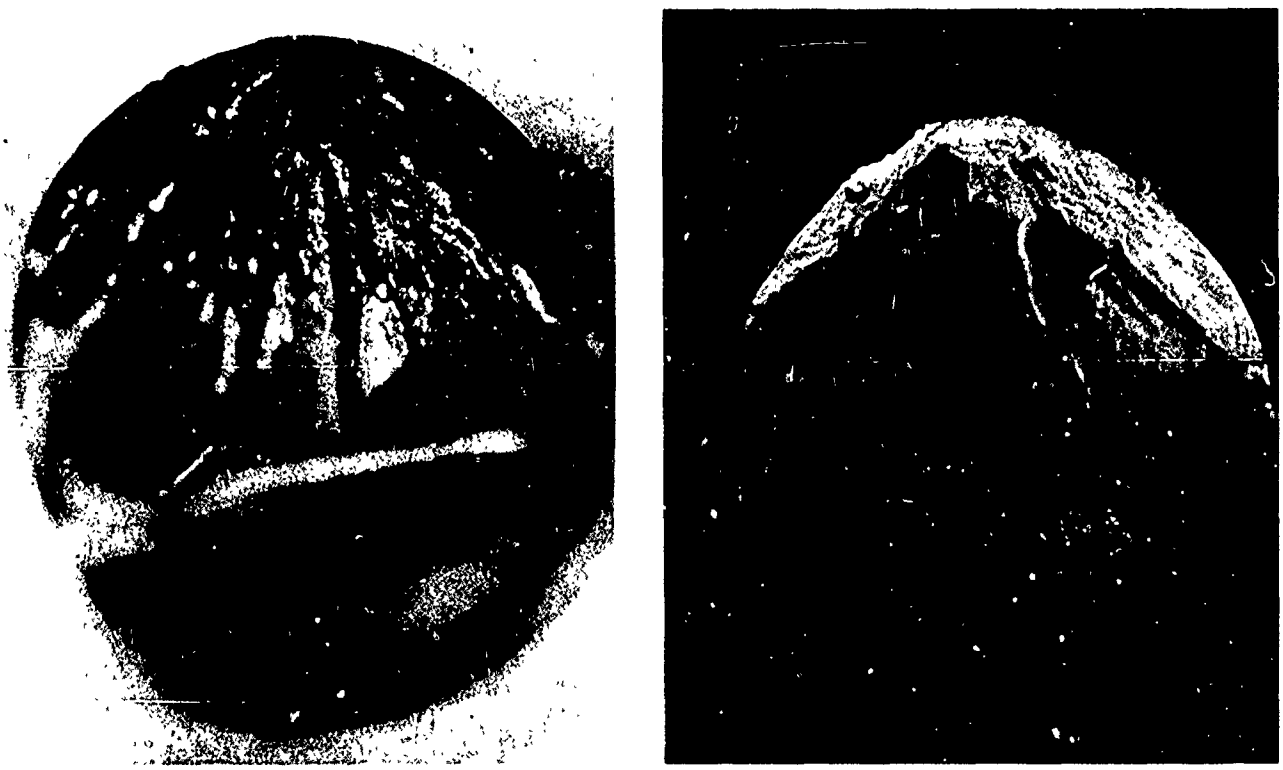

A. Optical Photomicrograph (27X)

B. Scanning Electron Micrograph (30X)

Figure 16 Fracture Surface of a strong specimen of 72% Al_2O_3-28% Cr_2O_3 (Billet No. 8-63-1)

to alumina, the strongest solid solution specimens were obtained at about 9-10 μm grain size where the strengths were about 70,000 psi. Although strictly comparable data are not available for alumina, our evaluation of the available evidence suggests that these solid solution specimens are stronger than alumina at this grain size. At the larger grain sizes where the advantage of reduced anisotropy was expected to be still more pronounced, difficulties in making bodies with good microstructures seem to have prevented the preparation of strong bodies.

IV. ESTIMATING THE RESIDUAL STRESSES IN QUENCHED ALUMINA FROM MIRROR DIMENSIONS

A. Introduction

Analysis of the fracture surfaces of polycrystalline ceramics has been handicapped by lack of an overall understanding of the fracture process. In many cases the fracture surfaces are flat and rather featureless. In these cases, it is difficult to locate fracture origins because several minor features may be present and there may be little or no evidence to indicate which feature is the critical flaw[25]. Heuer[26] has shown that fractures at high stresses in strong alumina show more features than those occurring at low stresses.

In contrast to polycrystalline ceramics, glass usually fractures with a fracture surface containing very well defined fracture features including the critical flaw, mirror and mirror boundary, hackle, and so forth. With these well defined features available, methods of analysis of the fracture surfaces have been extensively developed. Much attention has been focused on the study of mirrors. Terao[27], Levengood[28], and Shand[29,30] determined relationships between the breaking stress of glass and the dimensions of mirrors. Johnson and Holloway[31] have proposed an energy criterion for formation of the mirror boundary.

Kerper and Scuderi[32] investigated the mirror size vs. modulus of rupture for glasses of eight different compositions and found that the composition affected the mirror size. They concluded that the condition of the glass surface, the test temperature, difference in exposure time to test temperature, and rate of loading all effected the modulus of rupture but did not affect the relationship between the modulus of rupture and the mirror size. However,

the slope of the log-strength log-mirror radius curve decreases at low strength and large mirror size.

Whether or not a mirror is observed in the fracture surfaces of polycrystalline ceramics depends upon several factors some of which are not well understood at present. Shand[29] found that less detail was observable in the mirrors of polycrystalline glass ceramics compared with glass. He attributed this difference to the inhomogeneity inherent in polycrystalline bodies and stated that for certain ceramic materials, such as sintered alumina, with crystals still larger in size, no mirror at all is formed. However, whether or not a mirror is observed also depends upon other material properties and conditions. It may be that he failed to observe mirrors with alumina because the material was weak or the specimens were so small in cross section that the mirror boundary did not form within the dimensions of the fracture surface.

Recent improvements in the preparation of alumina ceramics, including the use of hot pressing to obtain dense, fine grained bodies and the use of compressive surface layers to obtain substantial increases in strength[33-35] have made available ceramics that form fracture surfaces with well defined features. Therefore, it is now possible to apply the techniques used to analyse the fracture surfaces of glass to the analysis of the fracture surfaces of polycrystalline ceramics.

In investigations of strength vs. mirror size in glass, it has been considered desirable to use specimens that are free of residual stress.[29] The reason for this is that the mirror size depends on the local stress (combined effect of stresses due to the applied load and residual stress, neglecting in this case the stresses due to crystal anisotropy because of the small volumes in which they are effective). Another possibility is to investigate specimens

with large scale residual stress and to use the difference between the nominal stress, calculated on the basis of the applied load, and the actual local stress as indicated by the mirror size to obtain an estimate of the magnitude of the residual stress. In this investigation this approach was used to obtain estimates of residual stresses in polycrystalline alumina specimens strengthened by quenching. These results were compared with the observed improvements in strength and the residual stresses calculated by Buessem and Gruver[36] based upon thermal stress calculations and creep data.

B. Fracture Stress vs. Mirror Size

Typical mirrors in fracture surfaces of alumina flexural strength test specimens are illustrated in Figure 17. The fracture surfaces are quite similar in appearance to those of glass rods. The fractures originated at surface flaws. As expected, the mirror size increases with decreasing strength. In addition, the other fracture features including hackle and flakes caused by crack branching become less pronounced.

The variation of mirror size with strength for normal loading rates is shown in Figure 18. The individual data points indicate results obtained with hot pressed alumina rods ranging from 0.09 to 0.15 in. in diameter. The dashed line represents data generously provided by R. W. Rice in advance of publication. These data were obtained using rectangular bars of 94, 96, 98 and 99+% alumina. Rice used intentional flaws to weaken some of the specimens in order to extend the curve to larger mirror sizes. The slope of the fracture stress vs. mirror size curve based upon Rice's data is approximately 0.40.

The slope of the curve based on the data from the present investigation is 0.46. Several investigators[28,31] of mirrors in glass have suggested the use of the relation

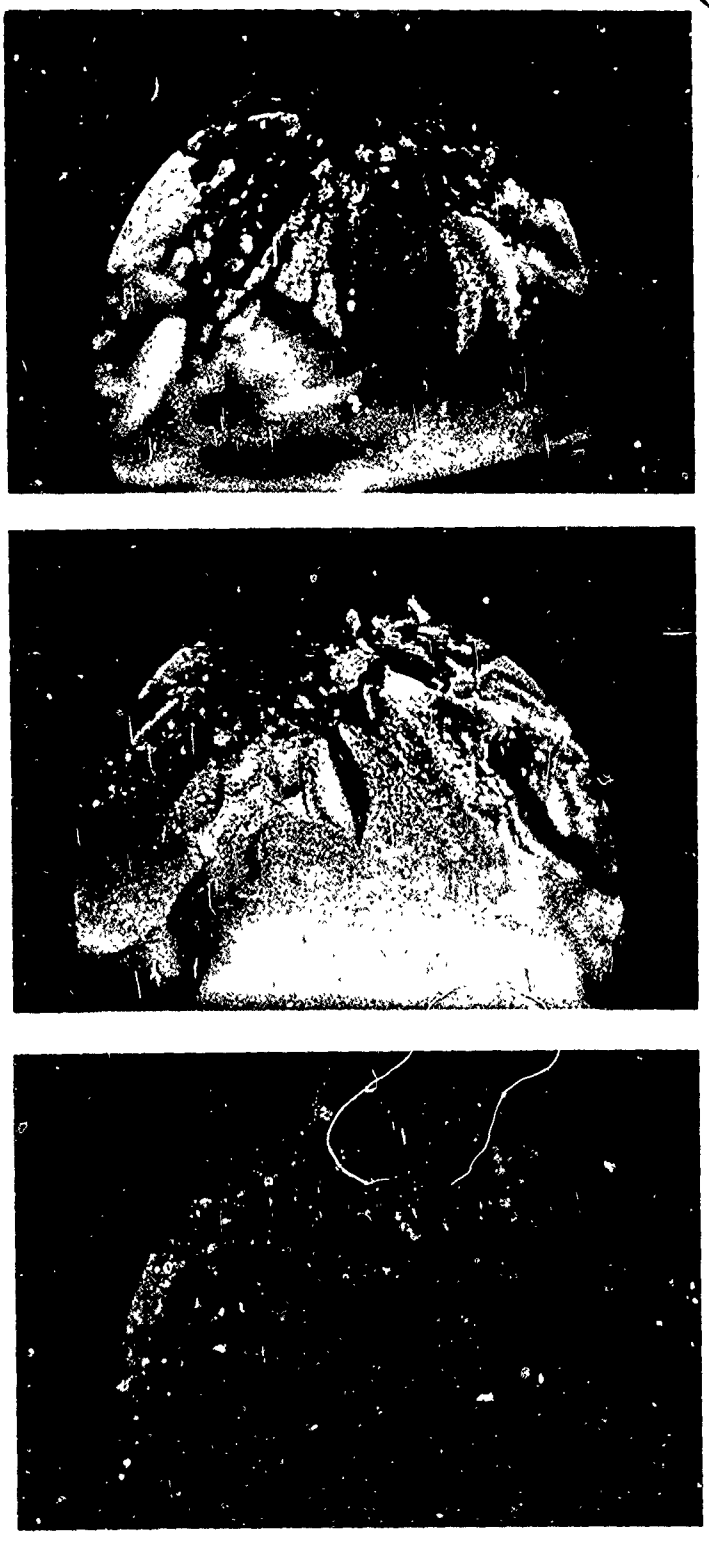

Figure 17 Fracture Surfaces of As Polished Alumina Rods in Which the Fractures Originated at Various Stresses at Surface Flaws (27 x)

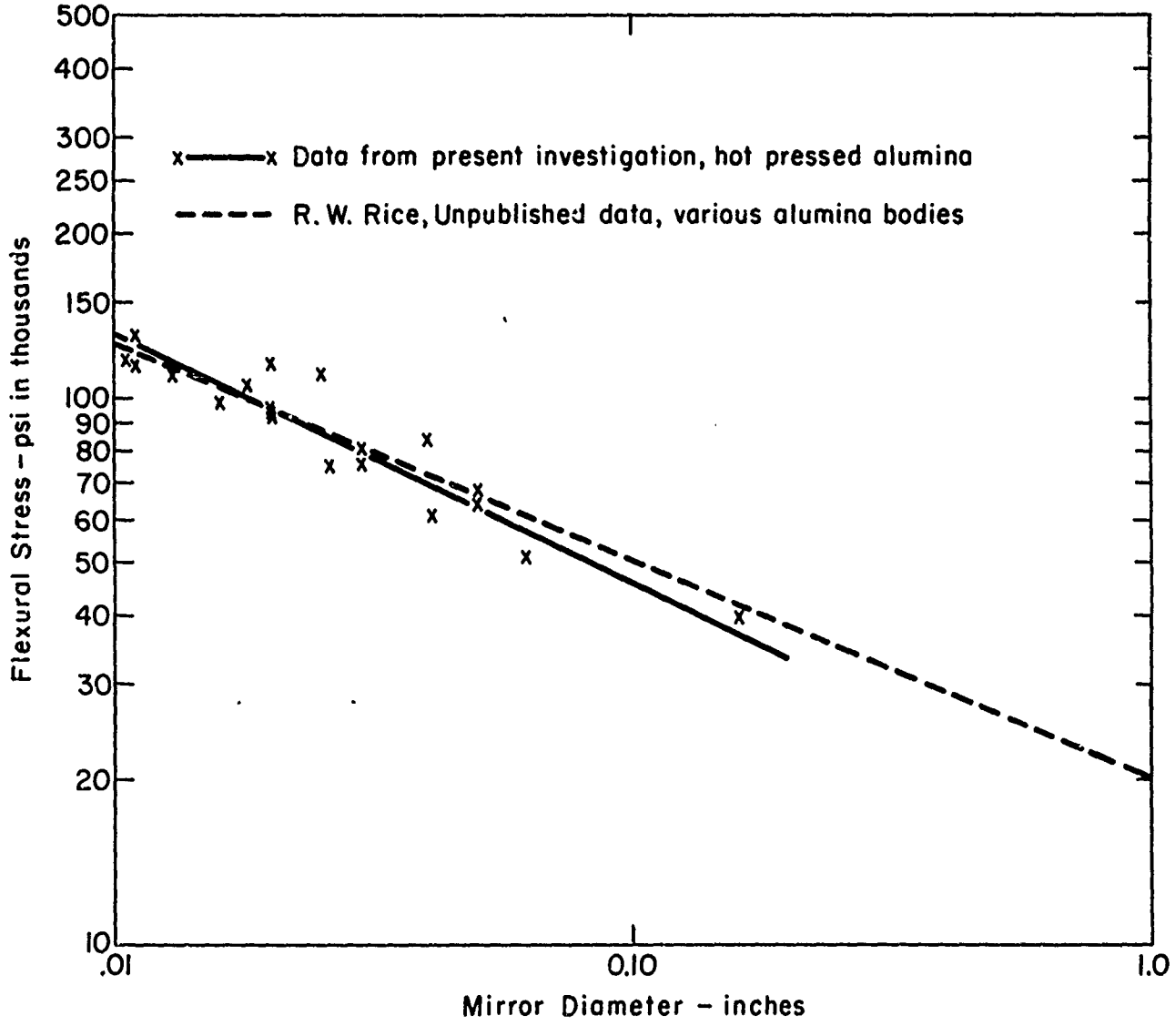

Figure 18 Stress at Fracture Origin vs. Mirror Diameter for Hot Pressed Alumina Rods

$$\sigma_f \, r_m^{1/2} = \text{constant}$$

to describe the relationship between the fracture stress (σ_f) and the mirror radius (r_m). However, after what appears to be the most comprehensive investigation of flexural strength vs. mirror size, Kerper and Scuderi[32] observed slopes that were usually substantially less than one half. The exponent approached one half for the strongest specimens (smallest mirrors). Thus, it seems possible that the lower slope is caused by the decrease in strain as the mirror boundary extends across the specimen in the flexural test. The factors that determine the location of the mirror boundary are not well understood. However, it does seem likely that the transfer of strain energy to the crack front is an important factor and in the case of large mirrors, strain energy from portions far removed from the crack front may influence the fracture.

Congleton et al[37,38] investigated crack branching in alumina. The exact relationship between crack branching and formation of the mirror boundary is uncertain but they seem to be closely related. These authors have proposed the following relation, again involving the exponent one half and assuming plane stress conditions:

$$\sigma_f \, c_b^{1/2} = 2 \left(\frac{E\gamma}{\pi}\right)^{1/2}$$

in which c_b is the crack length when branching occurs, E is Young's modulus and γ is the effective surface energy. Therefore, the observation of a slope of about one half is not unexpected. Since the average strength of the specimens used in the present investigation was substantially greater than Rice's, the greater slope can be accounted for on the same basis as in the case of the variations observed by Kerper and Scuderi.

The value of $\sigma_f r_m^{1/2}$ was calculated for the present data and found to be 8,300 lb $in^{-3/2}$ (9.1×10^8 dyne $cm^{-3/2}$). This value can be compared with a similar result for alumina (LUCALOX) obtained by Congleton and Petch using the radius at crack branching which was 7.3×10^8 dyne $cm^{-3/2}$. Since the radius at crack branching may be larger than the mirror radius, the actual difference may be greater than indicated by this comparison. Other factors that may influence the results are tensile vs. flexural loading and differences in specimen shape (thin plates vs. rods).

The mechanisms proposed by Congleton et al and Clark and Irwin[39] involve cracks that open up ahead of the main crack and that subsequently form the crack branches. At present this mechanism is not firmly established but it does seem reasonable that the Griffith condition applies in some way to the branches as well as the main crack so that the elastic modulus and the surface energy are expected to be important factors.

C. Estimating Residual Surface Stresses from Mirror Dimensions

A fracture surface showing a mirror with a diameter of 0.03 in. formed when the rod fractured at a stress of 80,000 psi is illustrated in Figure 19. This fracture surface is compared with another one having a mirror 0.03 in. in diameter obtained by breaking a rod strengthened by quenching from 1700°C into silicone oil (100 cs.) at a flexural stress of 141,800 psi. The similarities in mirror size and other fracture features are evident.

The mirror dimensions and the flexural strengths of rods quenched from 1550 and 1700°C were measured. Only fractures originating at the surface were used. The results are given in Table VIII and Figure 20. In Figure 20 the strength vs. mirror size curves for the quenched rods are compared with the results obtained for as polished rods.

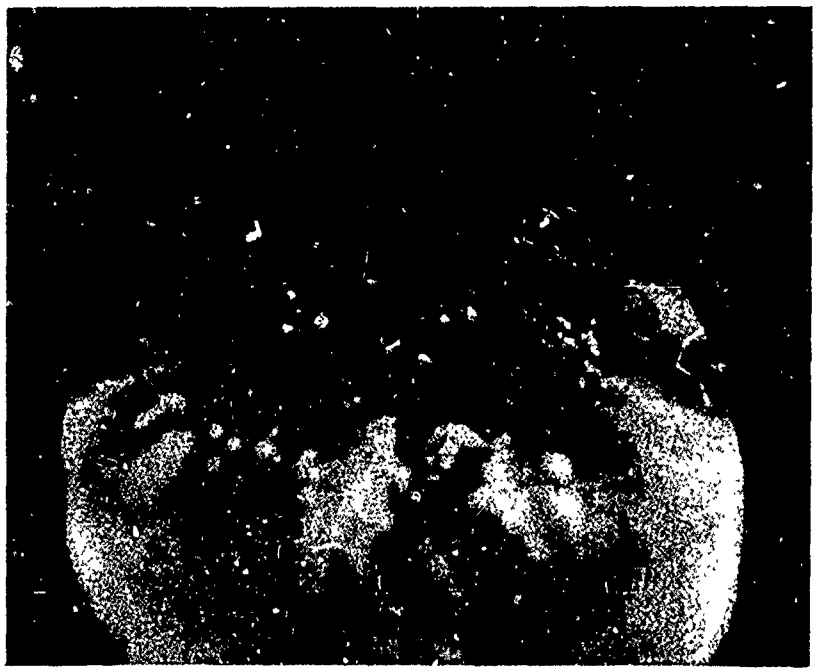

A. As Polished (80,000 psi)

100μm

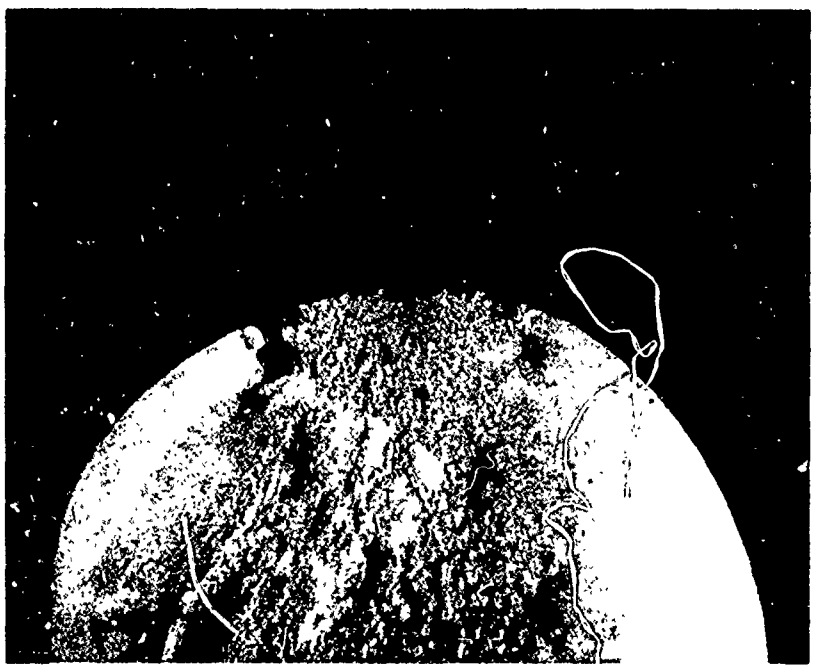

B. Quenched from 1700°C into silicone oil (141,800 psi)

Figure 19 Comparison of Mirrors in as polished and quenched Alumina Rods (27X)

TABLE VIII

Mirror Diameter and Strength of Hot Pressed Alumina Quenched in Silicone Oil (100 cs.)

Quenching Temperature °C	Mirror Diameter in.	Flexural Strength psi	Remarks
1550	0.015	154,400	small crack
	0.021	143,900	----
	0.022	132,700	----
	0.028	111,000	----
	0.038	104,500	large crack (tensile side)
1700	0.011	177,000	----
	0.020	160,500	----
	0.022	144,500	----
	0.030	141,800	----
	0.044	113,100	large flake

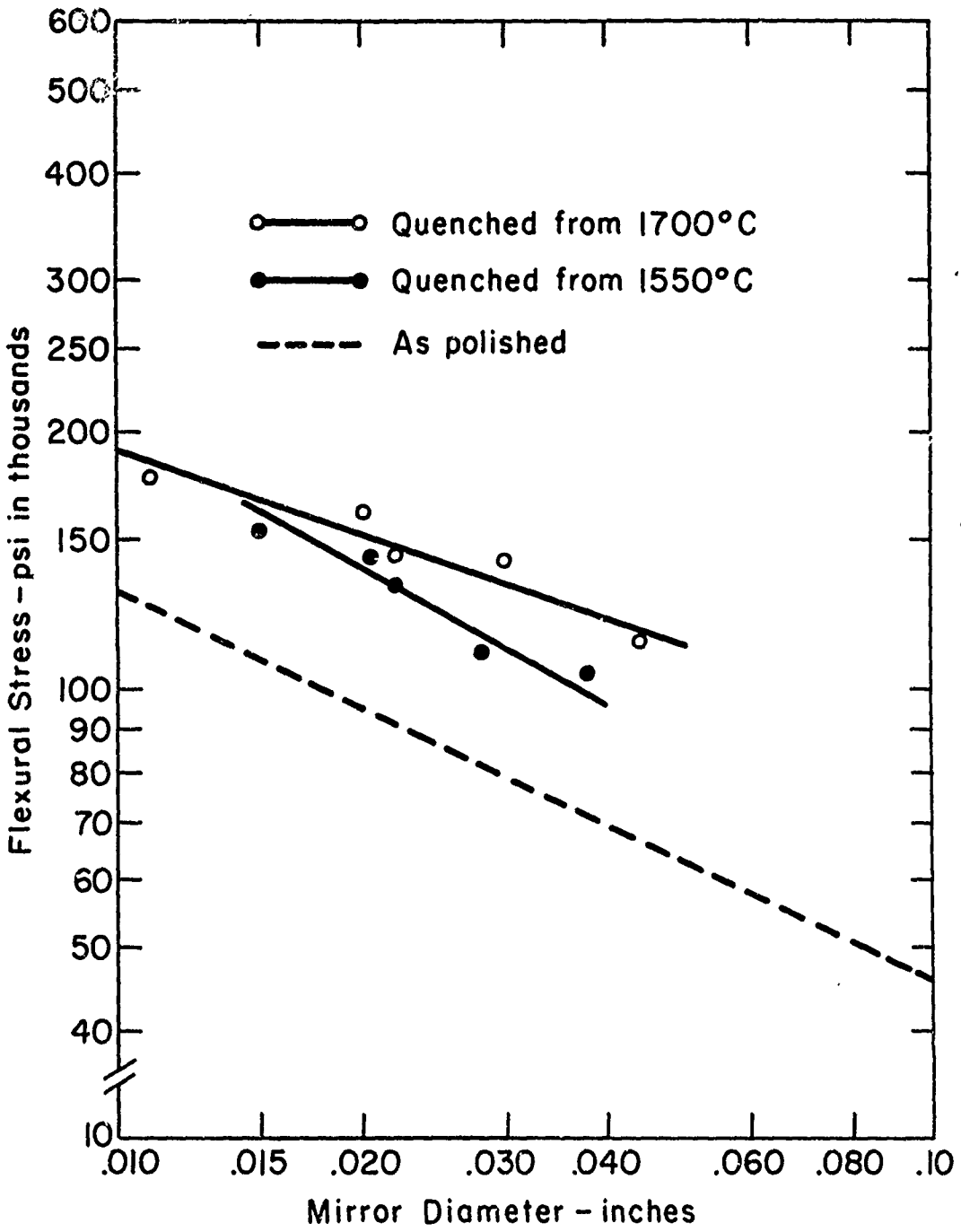

Figure 20 Stress at Fracture Origin vs. Mirror Diameter for Quenched Alumina Rods

Since the mirror size is determined by the local stress at which fracture occurred, all fractures at a particular mirror size actually occur at the same local stress. The curves for the quenched rods fall at higher stresses because the quenched rods support larger loads so that the nominal stresses calculated from the load and the rod dimensions are larger. The differences between the curves; that is, the differences between the nominal stresses in the quenched rods and those in the as polished rods are caused by the presence of the residual stresses and the magnitude of the difference provides an estimate of the residual stress.

At a mirror diameter of 0.020 in. the strength of an as polished rod is 94,000 psi. At the same mirror size the strength of a rod quenched from 1550°C is 138,000 psi. Thus, the residual stress in the surface of the quenched rod is approximately 44,000 psi. Similarly, the strength difference for rods quenched from 1700°C, taken at the same mirror size yields 58,000 as the estimate of the residual stress.

Since the differences between the curves remain approximately the same over a range of mirror size, the data indicate that the residual stresses present in the various rods quenched from a particular temperature are approximately the same in spite of the rather large variations in strength.

The present method of estimating the magnitude of the residual stresses is an improvement over comparing individual strength values for the following reasons:

1. The variations in the individual values are reduced by averaging.
2. Since all of the fractures originated at the surface, errors due to fractures originating in the interior are avoided.
3. Since the comparison is based on a physically significant fracture feature, changes other than residual stresses that may effect the strength may

not affect the estimated residual stress or
may effect it to a lesser degree.

The last item above raises the question whether or not the present data can be used to estimate the portion of the observed strengthening that should be attributed to the residual stresses and the portion that should be attributed to other causes such as reduction of precipitation[40]. In principal this can be done by comparing the difference in the average strength of a large group of quenched specimens in which the fractures originated at the surface and the average strength of a large group of controls with the strength increase expected based upon the estimated residual stresses. In the present specimens, a large fraction of the fractures originated at internal flaws so that too few specimens remained in each group to obtain the reliable average required for this comparison. However, it is evident that the principal reason for the improvement in strength is the residual compressive stress. In some of the stronger groups other factors may be making a minor contribution. In Sections D and E, some evidence for the existence of other strengthening mechanisms is presented.

Buessem and Gruver[36] calculated the residual stress profiles of 96% alumina rods quenched from 1500 and 1600°C. These calculations were done by numerical integration of equations for plastic strain using experimental heat transfer, creep and elastic modulus data. The calculated residual stresses at the surface were 17,900 psi for quenching from 1500°C and 29,500 psi for quenching from 1600°C. The measured flexural strengths were substantially greater than would be expected based upon the sum of the control strength and the calculated residual surface stress. Based upon these calculations it seems likely that inaccuracies in the assumptions and data lead to calculated residual stresses that are lower than those actually present.

It is not possible to make a direct comparison between the present residual stress estimates and those of Buessem and Gruver because of the differences in the heat transfer, creep, and elastic properties of the two materials. However, the present estimates do show that compressive stresses higher than those found by the calculations can be induced in alumina ceramics.

D. Failure at Internal Flaws

As polished rods usually fracture at surface flaws but in a few cases fractures have been observed to originate at internal flaws. One of these fractures is illustrated in Figure 21. In this case the calculated stress at the outer surface when fracture occurred was 110,800 psi. The fracture originated at a slightly lower stress about 0.010 in. from the surface. The fracture origin is visible as a diffuse, light colored spot at the center of the mirror.

In contrast to the as polished rods, the fractures in quenched rods usually originate at internal flaws. A number of these fracture origins were described previously[1,2].

During this investigation, the flexural strengths of the longest portions of some quenched specimens that were measured previously were measured again by three point loading on a 3/4 in. span. One of these specimens had a flexural strength of 223,000 psi, the highest individual strength value we have obtained so far for quenched alumina. The observed mirror is shown in Figure 22. The fracture originated internally at a point slightly more than half the distance from the surface to the axis. The mirror is small, approximately circular, and bounded by surface roughness and small flakes. The fracture surface is distinctive mainly because of the sharpness of the radiating ridges and the flatness of the radiating valleys shown in Figure 22B.

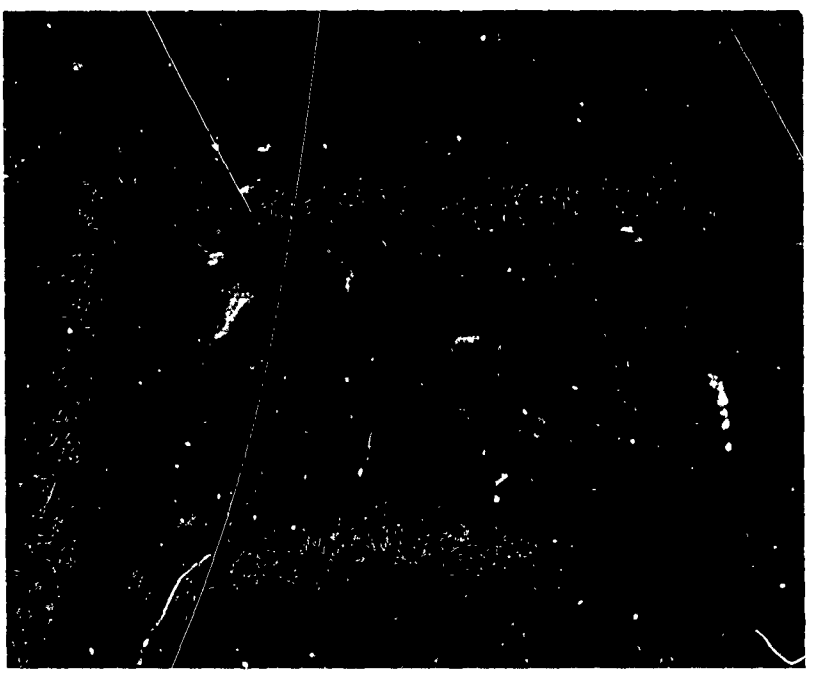

Figure 21 Fracture surface showing an internal fracture origin (27X)

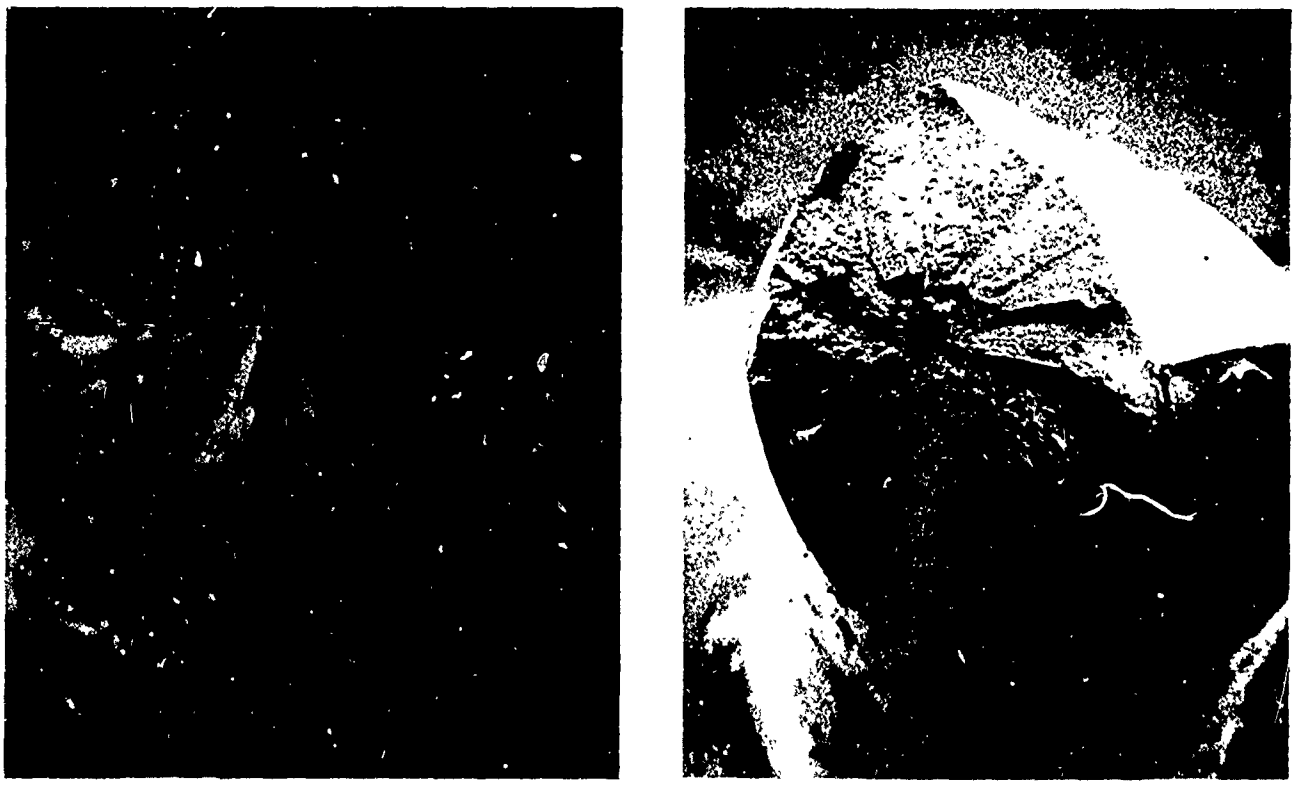

A. Optical Photomicrograph
27X

B. Scanning Electron Micrograph
30X

100μm

Figure 22 Mirror observed in quenched specimen fractured at a nominal stress of 223,000 psi (quenching temperature 1700°C, 100 cs. silicone oil)

The fracture origin of this strong rod is illustrated in Figure 23A. The nature of the flaw is not readily apparent but it may be an irregularly shaped pore or porous region with some slightly larger than normal grains associated with it.

The flaw size is approximately 25 μm, much larger than the average grain size. This observation is consistent with many previous observations of flaws in strong, fine grained alumina.

The texture of the fracture surface within the mirror is shown in Figure 23B. The fracture is almost entirely intergranular. The uniformly small grain size (average grain size $\cong$ 1 μm) and well formed grains and facets are evident. The texture of the fracture surface in the flat portion of one of the radiating valleys is shown in Figure 23C. This surface is quite similar to the mirror except that there are some larger areas of transgranular fracture.

The mirrors observed in fractures originating at internal flaws are described in Table IX. The data are not very conclusive at this point because of the small number of mirrors that have been measured and the possibility that those selected for measurement are not representative of all of the specimens that have been used in these experiments. Nevertheless, these observations indicate some interesting possibilities. The stress at the flaw was estimated in each case based upon the mirror size, using the strength vs. mirror size curve in Figure 18. The stresses, acting locally at the flaws, and necessary to cause failure are higher in the case of specimens quenched from 1700°C than for those that were not quenched or were quenched from 1550°C. Thus, it might appear that the material in the interior of the specimens is actually strengthened either by reheating or rapid cooling. Another possibility is that this difference in mirror size is

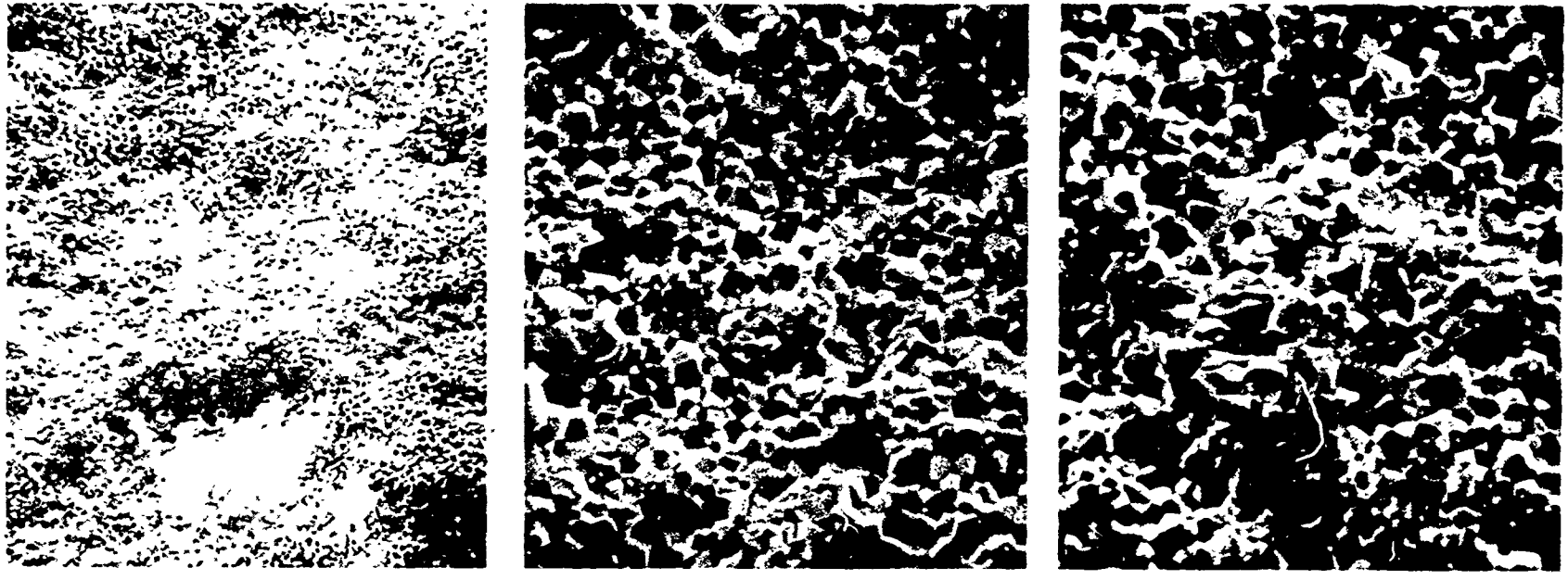

A. Fracture Origin
1000X
10μm

B. Fracture Surface in Mirror
3000X

C. Fracture Surface Outside Mirror
3000X
1μm

Figure 23 Fracture surface of quenched specimen fractured at a nominal stress of 223,000 psi (quenching temperature 1700°C, 100 cs. silicone oil)

TABLE IX

Characterization of Mirrors for Fractures Originating at Internal Flaws

Billet No.	Quenching* Temp. °C	Rod Diameter in.	Mirror Diameter in.	Flaw Distance from Axis in.	Flexural Strength psi	Stress at Flaw** psi	Description of Flaw
8-9-1	none	.132	.017	.055	110,800	102,000	----
8-62	none	.085	.020	.038	110,600	95,000	----
8-33-1	1550	.138	.024	.046	129,200	87,000	large pore
8-34-1	1550	.139	.028	.047	129,800	81,000	black spot
8-12	1700	.120	.010	.040	129,400	125,000	----
8-11	1700	.147	.011	.032	223,000	120,000	----
8-11	1700	.147	.011	.047	156,700	120,000	----
8-12	1700	.145	.020	.052	133,400	95,000	----
8-12	1700	.145	.010	.057	123,700	125,000	----
8-54	1700	.114	.010	.037	144,100	125,000	large pore

* Quenched rods were quenched in silicone oil (100 cs.)

** These stresses were estimated based upon mirror diameter using Figure 18.

influenced by the presence of other stresses. This will be discussed further in a later section.

Another observation is that the relative distance of the center of the mirror from the axis varies with the strength. The relative distances were calculated by dividing the distance of the flaw from the axis by the rod radius. These results are plotted in Figure 24 which indicates a definite correlation between the two variables.

E. Fracture Stress vs. Mirror Size at Elevated Temperatures

The possibility of an effect of temperature on mirror size was considered. Kerper and Scuderi[32] show that the mirror size of glass does not vary with temperature other than the variation accounted for by the variation of fracture stress with temperature. The mirrors of rods fractured in flexure at various temperatures were measured and compared with those observed at room temperature. The flexural strength and mirror size data are presented in Table X and plotted vs. temperature in Figure 25. In a rough way the strength decreases as the mirror size increases and vice versa. This variation would be expected if $\sigma_f r_m^{1/2}$ = constant applies at elevated temperature as well as at room temperature. The calculations show that $\sigma_f r_m^{1/2}$ is approximately constant except for the values at 200 and 300°C. In these two cases, the mirrors seem larger than expected.

The elevated temperature mirror sizes are compared with those expected at the same strength using room temperature data in Figure 26. At first glance it seems that the elevated temperature data are scattered almost equally about the line representing the room temperature data. However, when the data from 200 and 300°C are separated from the rest of the data, it is evident that the elevated temperature values are lower in strength at a given mirror size than would be expected at room temperature. Since both the Young's modulus and the surface energy decrease slowly with

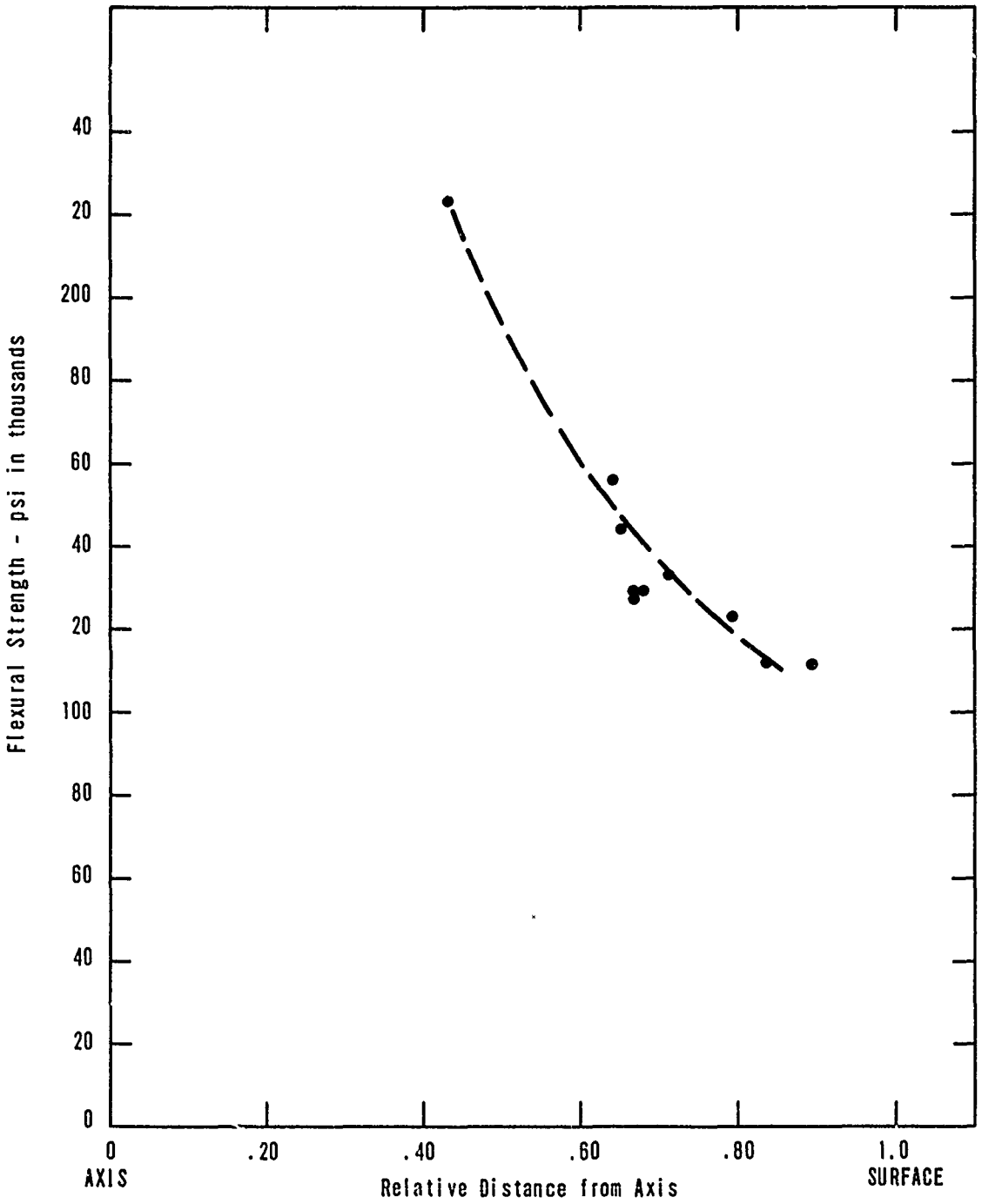

Figure 24 Flexural Strength vs. Distance of Fracture Origin from Rod Axis

TABLE X

Mirror Diameter and Elevated Temperature Strength

Testing Temperature °C	Mirror Diameter in.	Flexural Strength psi	$\sigma_f r_m^{1/2}$ lb.in.$^{-3/2}$	Flaw Location
		As Polished Rods		
25	0.020	94,000	9,400	edge flaw
200	0.035	90,000	11,800	edge flaw
300	0.035	78,000	10,300	edge flaw
400	0.035	72,000	9,500	edge flaw
500	0.030	65,000	8,000	edge flaw
600	0.030	80,000	9,800	edge flaw
800	0.030	75,000	9,200	edge flaw
900	0.023	84,000	9,000	edge flaw
1000	0.025	72,000	8,100	edge flaw
1100	0.025	78,000	8,800	edge flaw
1200	0.040	70,000	9,900	edge flaw
1300	0.038	58,000	8,100	edge flaw
1400	0.120	40,000	9,800	edge flaw
1500	---	specimen bent	--	
		Quenched from 1550°C in Silicone Oil (100 cs.)		
25	0.020	145,000	---	edge and internal
500	0.020	110,000	---	edge flaw
800	0.015	125,000	---	edge flaw
1000	0.015	115,000	---	edge and internal
1100	0.020	82,000	---	edge and internal
1200	0.020	60,000	---	internal flaw
1300	0.015	35,000	---	internal flaw

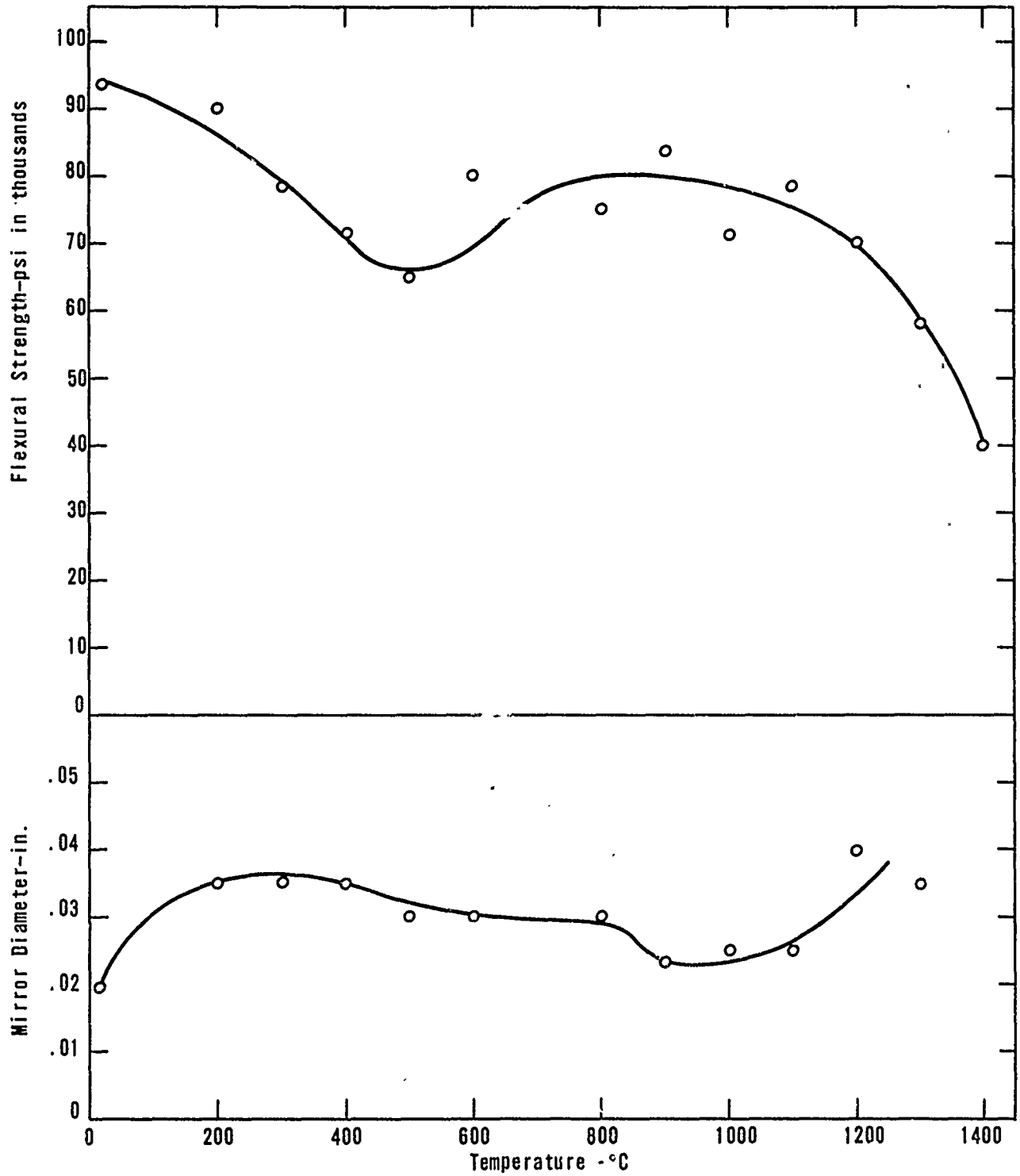

Figure 25 Mirror Diameter and Flexural Strength vs. Testing Temperature for Hot Pressed Alumina Rods

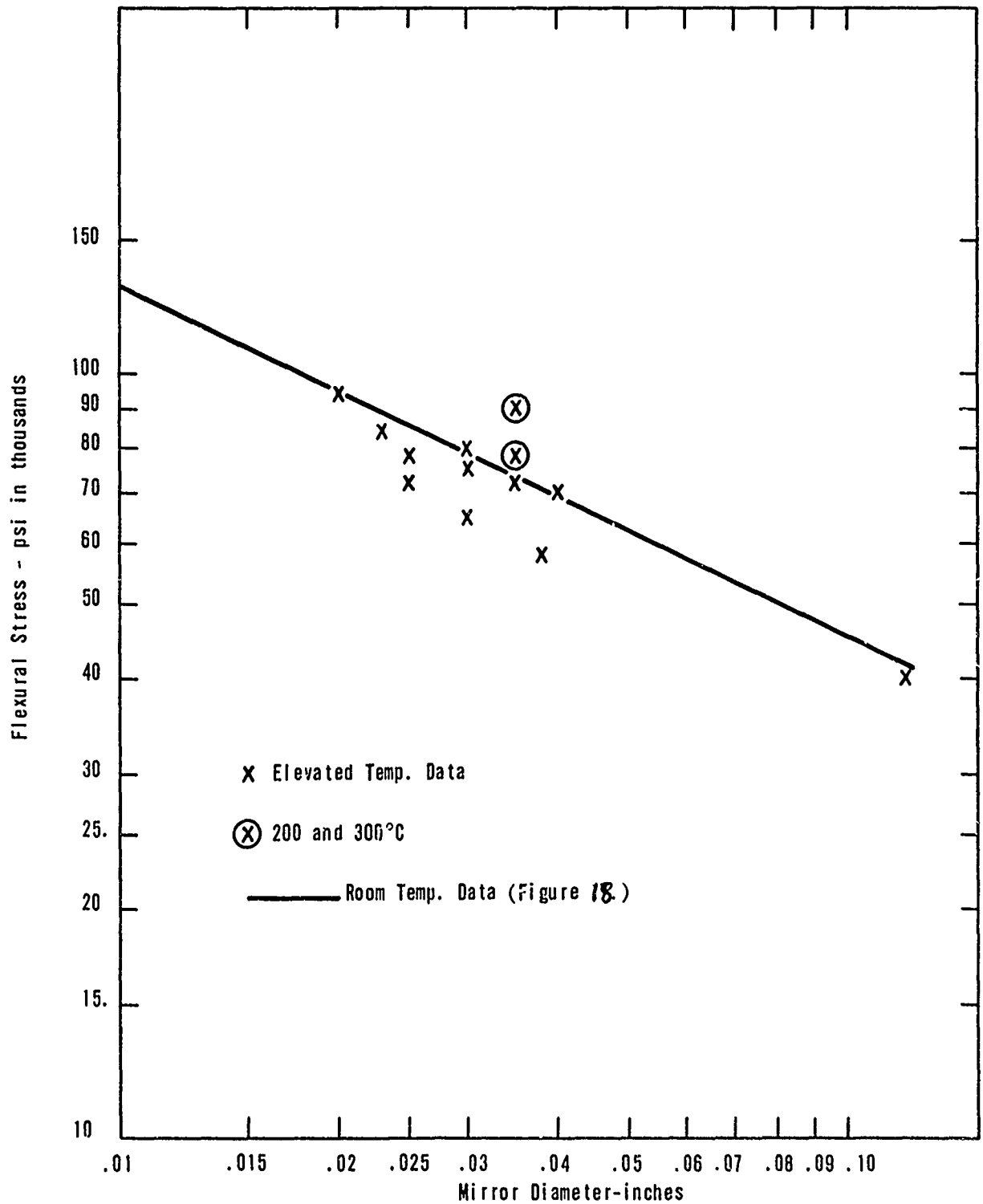

Figure 26 Flexural Stress vs. Mirror Size for Elevated Temperature Fractures

increasing temperature this variation might have been expected based upon the Congleton and Petch equation.

It has been evident for some time that it would be desirable to have a measure of the relative effect of microplasticity on the fracture energy. According to Ryshkewitch[41] the surface tension of molten alumina is estimated to be 900 dynes cm^{-1}. The surface tension increases with decreasing temperature at a rate of about 0.1 dyne cm^{-1} per degree C so that at room temperature it is about 1100 dyne cm^{-1}. Measured fracture energies are one to two orders of magnitude larger.

Many claims have been made that all or most of the difference between the surface energy and the fracture energy in brittle ceramics can be accounted for by microplasticity. If this is the case, it may be reasonable to expect an increase in fracture energy as temperature increases because of the substantial increase in the amount of plastic flow. The effective surface energy for fracture initiation of UO_2 does increase substantially with increasing temperature[42] but those of MgO[43] and Si_3N_4[44] change only slightly. Available information for a rather coarse grained alumina body indicates a decrease from 24,000 dyne cm^{-1} at 20°C to 15,000 dyne cm^{-1} at 1000°C[45]. On the other hand Congleton, Petch and Shiels[38] show a decrease from 30,000 dyne cm^{-1} at -200°C to about 15,000 dyne cm^{-1} at 250°C followed by an increase to 60,000 dyne cm^{-1} at 500°C for LUCALOX. Thus, it appears that there is no general increase in fracture energy with temperature in polycrystalline ceramics.

Since E and σ_f of alumina change only slightly with increasing temperature, the equation of Congleton and Petch predicts that, if γ increases substantially with increasing temperature, increasing mirror size will be observed.

The temperature variations of $\sigma_f r_m^{1/2}$ and $2\left(\frac{E\gamma}{\pi}\right)^{1/2}$ are plotted in Figure 27. In these calculations, values of E,

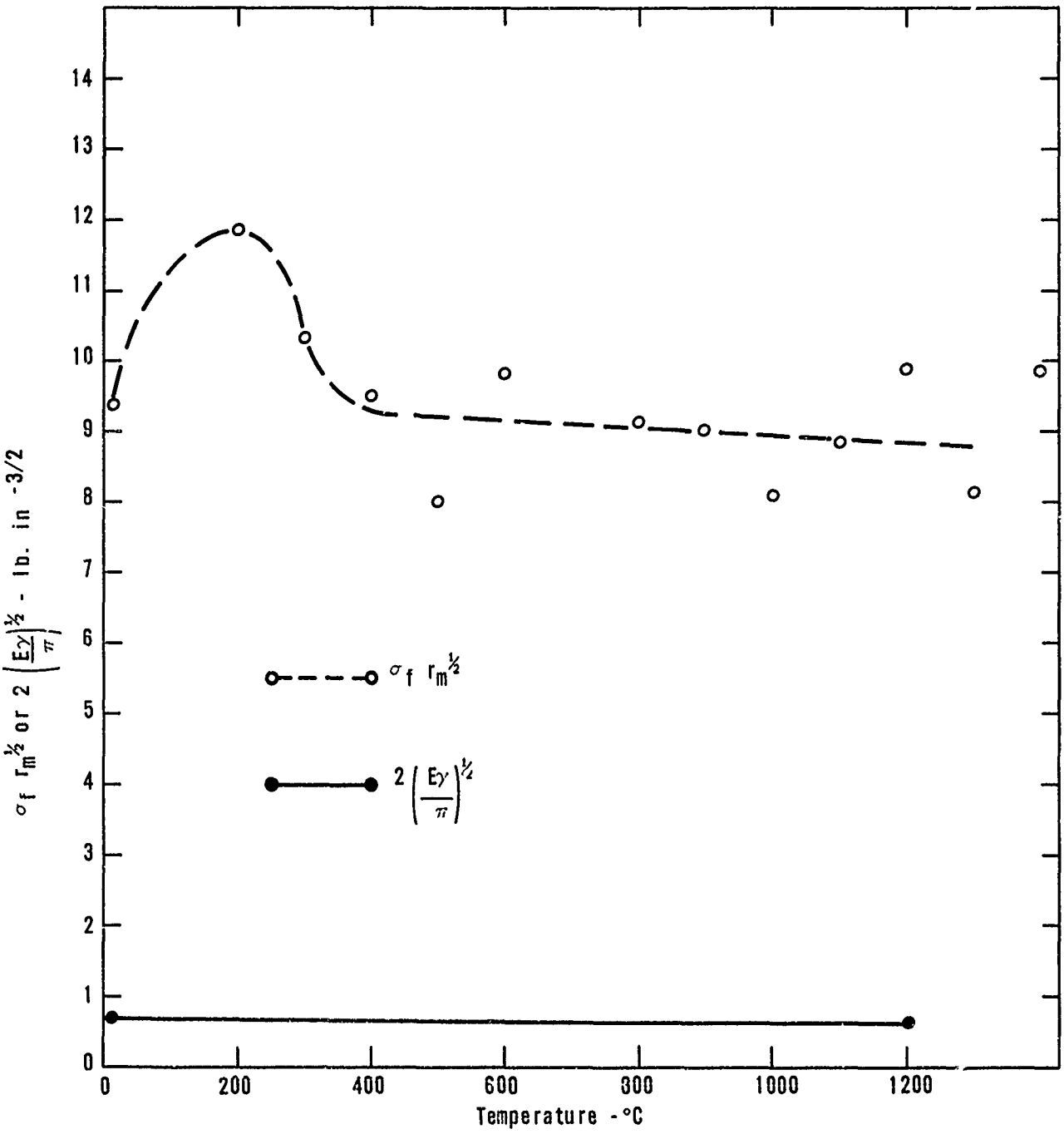

Figure 27 Variation of $\sigma_f r_m^{1/2}$ and $2\left(\frac{E\gamma}{\pi}\right)^{1/2}$ vs. Temperature

obtained by dynamic methods, were taken from Lynch et al[46] and γ was based upon estimates from Ryshkewitch[41]. This calculation leads to lower values than those obtained by Congleton and Petch because of the lower value of γ.

Comparing the two curves, it is evident that, except for the values at 200 and 300°C there is little variation with temperature and if the lower curve were multiplied by a constant factor of about 14 it would roughly coincide with the upper curve.

It seems likely that the discontinuity in $\sigma_f r_m^{1/2}$ at 200°C is a real effect. The strength is normal and the difference in mirror size seems too great to be attributed to experimental error. Further investigation of this discontinuity may produce evidence of the factors affecting the fracture mechanism in this temperature range.

The principal interest in the variation of $\sigma_f r_m^{1/2}$ with temperature lies in the possibility that it may provide evidence of the role of microplasticity in the fracture of these brittle materials. It seems reasonable to expect that, at particular temperatures at which various microplastic processes can occur, they would cause large variations in γ, thus causing variations in $\sigma_f r_m^{1/2}$ as indicated by the equation of Congleton and Petch. The present evidence indicates that these effects are absent, especially at high temperatures where they might be expected to have their greatest effect. This observation casts doubt on the conventional theory that the effective fracture energy is one or two orders of magnitude greater than the surface energy because of increases in γ due to plasticity. Even at 1400°C, just below 1500°C where the alumina deforms without breaking, $\sigma_f r_m^{1/2}$ has a normal value.

The flexural strength and mirror diameter of the quenched alumina specimens are plotted vs. temperature in Figure 28. The data are fragmentary. Also, the results include fractures

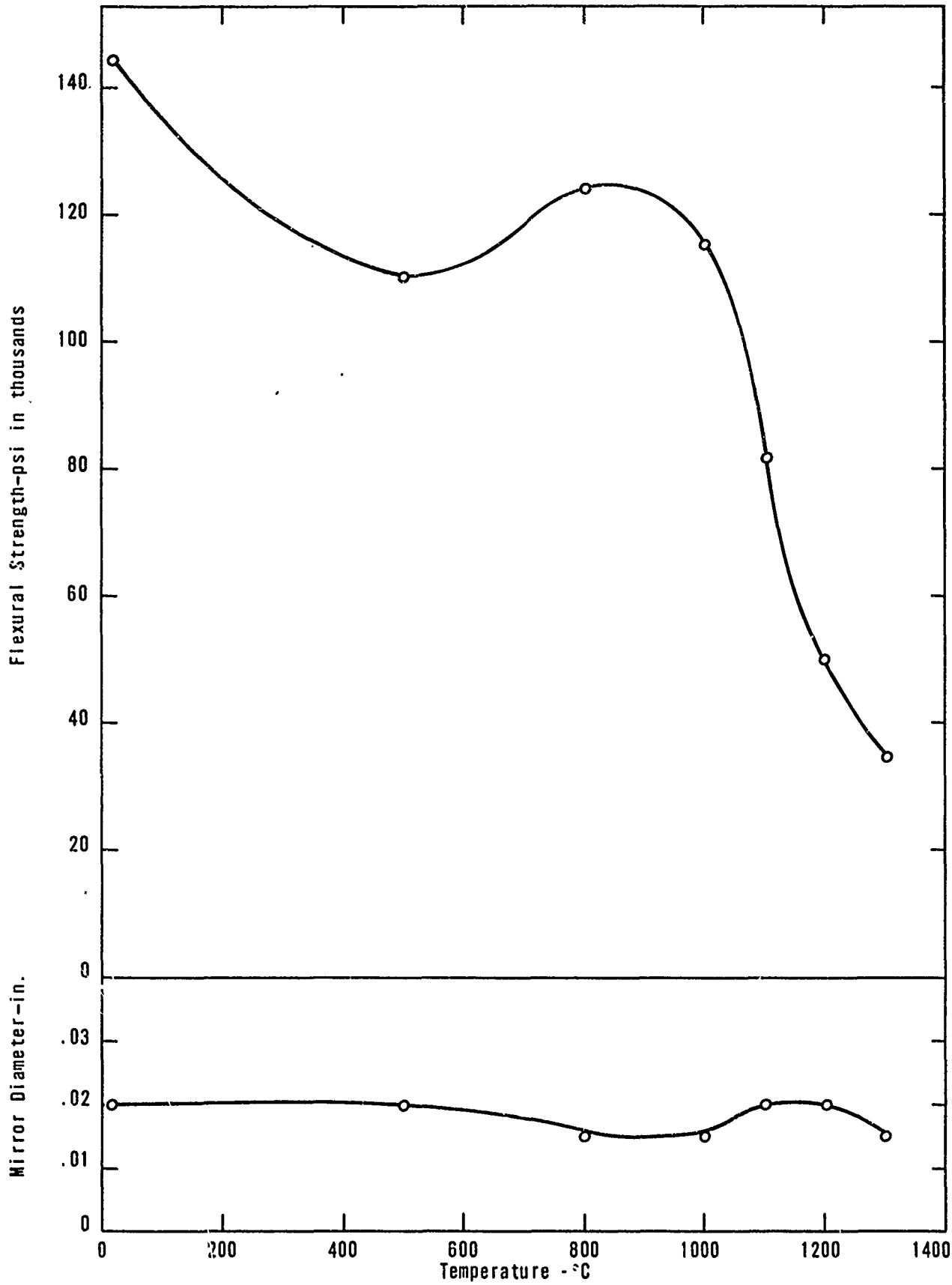

Figure 28 Mirror Diameter and Flexural Strength vs. Testing Temperature for Hot Pressed Alumina Rods Quenched from 1550°C into Silicone Oil (100 CS.)

at internal flaws and residual stresses are present so that the calculated strength does not represent the stress acting at the flaw. For these reasons interpretation of these results is difficult.

One notable factor is that the average mirror size is smaller than in the case of the as polished rods. This observation indicates that the local stress acting at the flaws in the quenched specimens is greater than in the case of as polished rods, both for surface and internal flaws. This, in turn, suggests that another strengthening mechanism, in addition to the compressive surface layers, is contributing to the high strengths.

F. Residual Stress Near Rod Axis

Hot pressed rods that are severely quenched fracture spontaneously when they are reheated to 1100-1200°C[2]. These fractures usually originate near the rod axis. The mirrors at these fracture origins were measured and the stresses at the fracture origins were estimated using the strength vs. mirror size curve at room temperature. The most frequent stress at or near the axis was 76,000 psi. Figure 29 illustrates one of these mirrors. The individual mirror sizes and estimated stresses are listed in Table XI. Because there is no applied load, the stress at which the spontaneous fracture occurs is the strength of the local material under those conditions. Therefore, the strength of the material at the axis is about 76,000 psi in the temperature range 1100-1200°C. This value agrees approximately with the flexural strength of as polished alumina in this temperature range. Therefore, in contrast to the behavior at lower temperatures, above 1100°C the surface and the interior of the alumina have approximately the same strength.

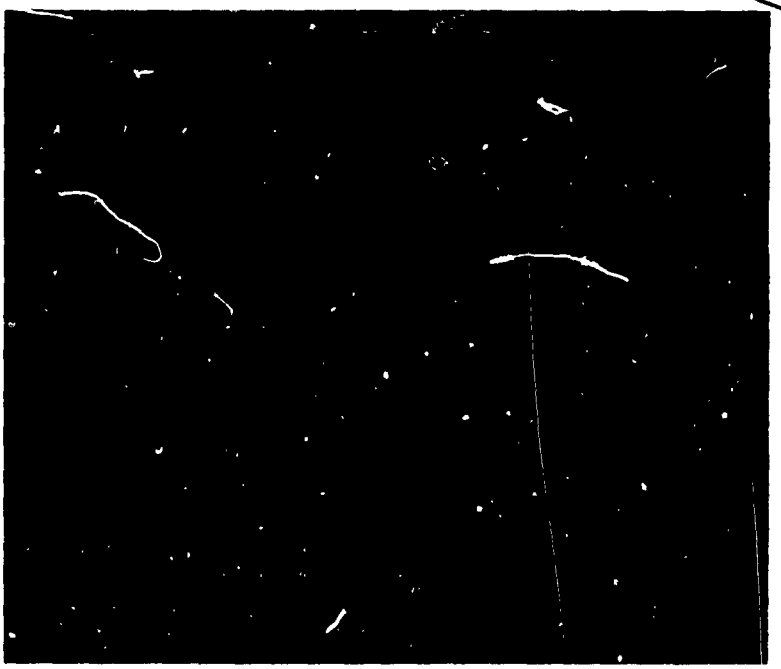

H
100 µm

Figure 29 Fracture Surface of Severely Quenched Alumina Rod which fractured spontaneously on reheating to 1100-1200°C (21X)

TABLE XI

Estimates of Axial Stresses Based on Mirror Dimensions at Spontaneous Fractures

Rod Diameter in.	Relative Distance from Axis to Flaw	Mirror Diameter in.	Estimated Stress from Figure 18* psi
0.154	0.03	0.015	106,000
0.148	0.03	0.050	76,000
0.141	0.07	0.030	76,000
0.142	0.80	0.030	76,000
0.150	0.15	0.030	76,000
0.143	0.02	0.030	76,000
0.130	at edge	0.040	68,000
0.138	at axis	0.138	36,000
0.140	at axis	0.140	37,000
0.142	at axis	0.142	37,000

* Note that these values are not corrected for the variation of mirror size with temperature. It is likely that such a correction would reduce these values by 5,000-10,000 psi.

G. Residual Stress Profile

A residual stress profile for specimens quenched from 1700°C into silicone oil (100 cs.) was constructed based upon the following information and conditions.

1. The residual compressive stress at the surface is 58,000 psi (from Figure 20)
2. The residual tensile stress at the axis is 76,000 psi (from Table XI)
3. The volume averaged residual stress is zero.
4. The general shape of the stress profile is similar to those of Buessem and Gruver[36].

The stress profile is presented in Figure 30. Comparing this stress profile with those calculated by Buessem and Gruver for quenching from 1500 and 1600°C shows reasonable increases in surface compressive stresses with increasing quenching temperature. The residual tensile stress at the axis is less than might be expected from the calculations but this may result from the differences in the materials.

It is interesting to estimate the local stress at failure for the specimens failing at internal flaws by combining the residual stress profile and the local stresses due to the applied load. The results are plotted in the upper right hand quadrant of Figure 30 and show a monotonic decrease in strength with distance from the rod axis. The low values occur in the region of greatest slope in the stress profile suggesting that the other principal stresses (radial, circumferential) have a role in these failures.

These local stresses can be compared with the local stresses based on the mirror dimensions which are listed in Table IX. It may be possible to reconcile the differences between the two groups by taking the other principal stresses into account.

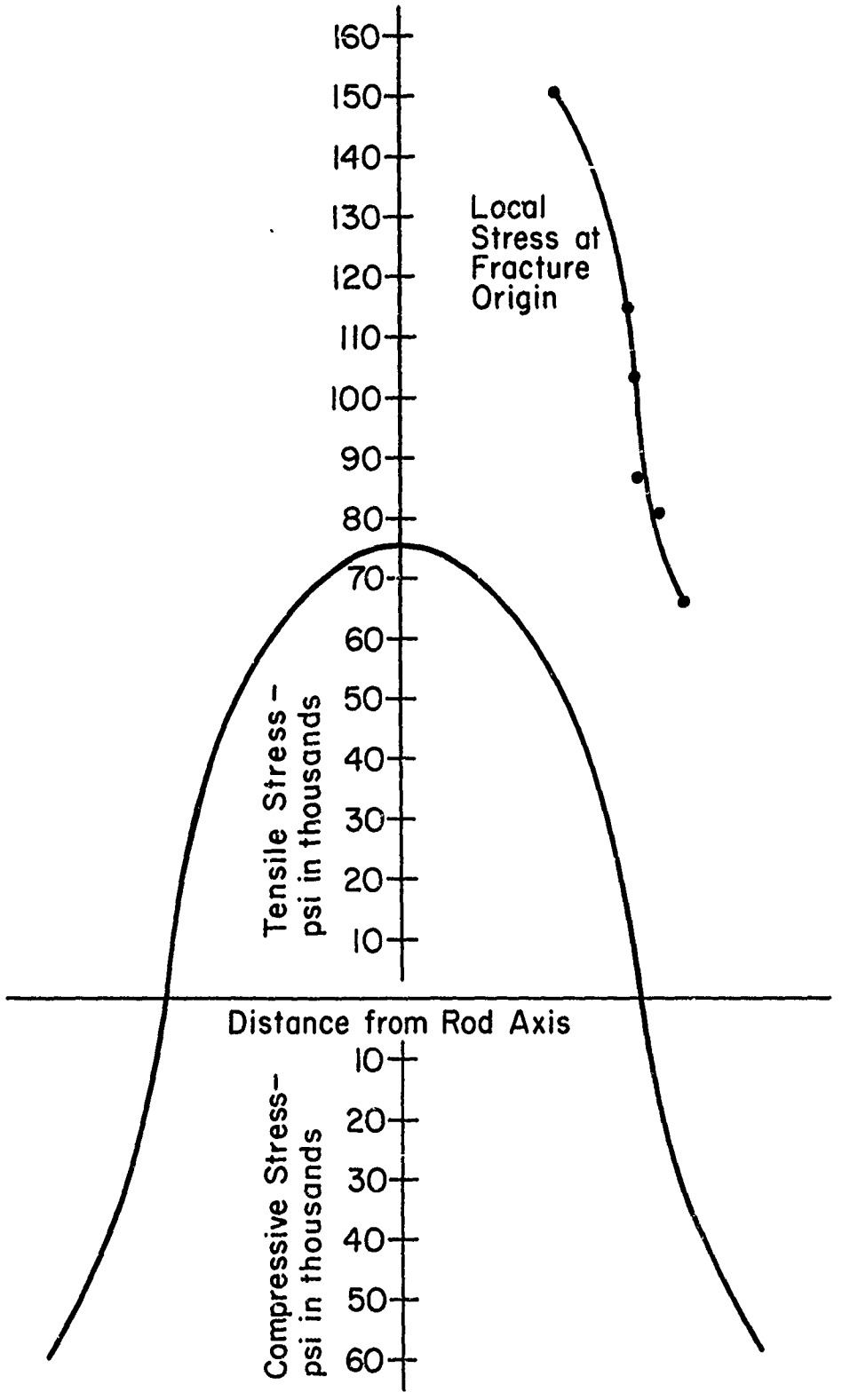

Figure 30 Estimated Stress Profile for Hot Pressed Alumina Rods Quenched from 1700°C into Silicone Oil (100cs.).

The stresses acting at fracture in as polished and quenched rods are compared in Figure 31. The particular rods chosen for comparison are those illustrated in Figure 19 that showed approximately equal mirror dimensions. The total strain energy is not directly proportional to the stress curves because the rods are cylindrical, not rectangular. However, it is evident that the tensile strain energy in the quenched rod is more than twice that of the unquenched rod. Since the mirror dimensions are the same in both cases, it is reasonable to conclude that either the strain energy is not an important factor or the strain energy around the fracture origin is the only part that affects the mirror formation. It seems likely that tensile strain energy from regions remote from the mirror does not affect the mirror formation.

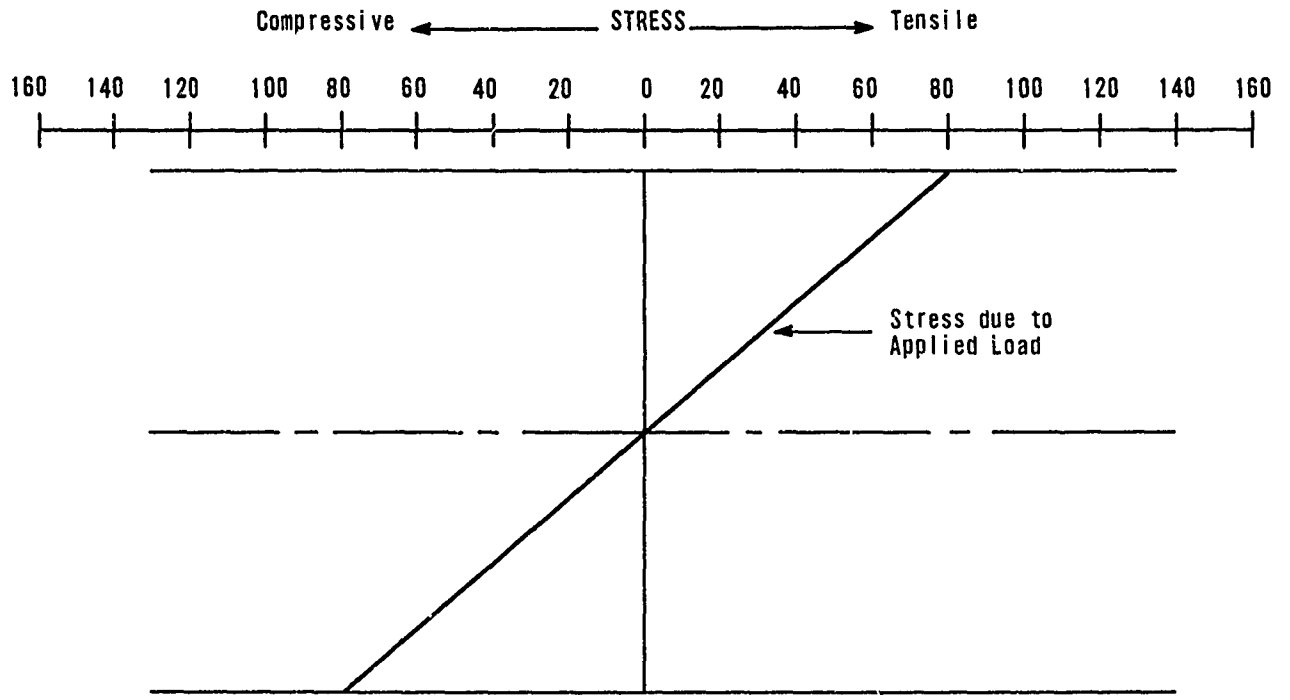

A. As polished, 80,000 psi

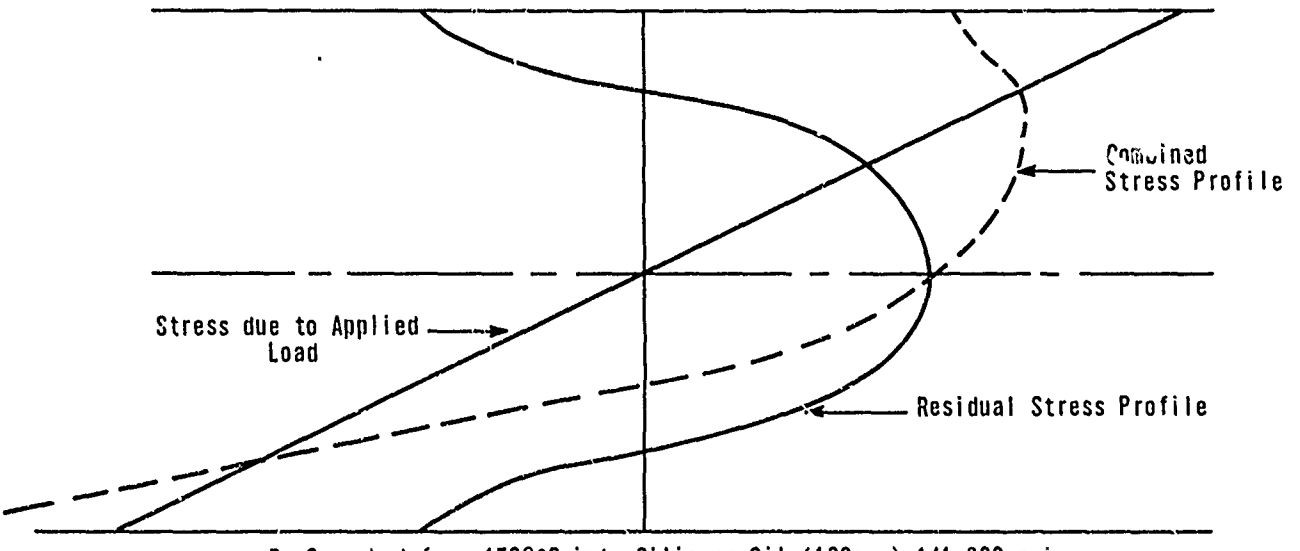

B. Quenched from 1700°C into Silicone Oil (100cs.) 141,800 psi.

Figure 31 Comparison of Stresses Acting in As Polished and Quenched Rods with Approximately Equal Mirror Dimensions

V. SUMMARY AND CONCLUSIONS

Strengthening by Reduction of Crystal Anisotropy

Polycrystalline ceramic bodies composed of crystals with reduced anisotropy were prepared by hot pressing compositions in the system Al_2O_3-Cr_2O_3. The heating rates that were used were lower than those used previously. Using the lower heating rates made it possible to prepare specimens with average grain sizes as large as 57 μm compared with a maximum of 20 μm obtained previously. It seems likely that the slower heating rates allow removal of pores at lower temperatures so that upon subsequent heating at higher temperatures the pores are not present to inhibit grain growth.

The reaction to form the solid solution was essentially complete after two hours at 1325°C. Fine grained bodies were obtained with this heat treatment. Coarse grained bodies were made by hot pressing at higher temperatures for longer periods of time. After heating at 1650°C for five hours the average grain size was 57 μm.

The grains in the fine grained bodies were slightly elongated. As the pressing temperatures were raised in order to make coarser grained bodies, large lathlike crystals were observed. These crystals are similar to those observed in alumina bodies. At the highest pressing temperatures, the microstructures changed again so that the material consisted of rounded grains with a bimodal grain size distribution. Magnesia is effective as a grain growth inhibitor.

The variation of strength with composition (Cr_2O_3 content) was investigated for coarse grained compositions ranging from seven to 28% Cr_2O_3. The highest average strength was obtained at 21% Cr_2O_3.

The strength vs. grain size of 72% Al_2O_3-28% Cr_2O_3 and similar compositions with additions of 0.1 and 0.25% MgO were measured. Some strong, fine grained specimens were made. The hignest individual strength value was 118,000 psi. Even though this is ccnsidered to be a strong body, similar high strengths have been observed with strong fine grained alumina.

The strength decreases with increasing grain size as expected. Considering all the evidence from this research and that reported earlier,[4,21] there seems to be only small grain size dependence of strength in the grain size range from 0.35 μm to 10 μm. At the very fine grain size end of this range, the strengths may be lower than otherwise expected because of failure to achieve full density or lack of sufficient heat treatment to form a strong bond between the grains. However, good densities and high strengths were achieved at 0.9 μm. From 0.9 μm to 10 μm the slope of the strength vs. grain size curve varies from 0.15 to 0.31, depending upon the particular set of data used. If the slope of the strength-grain size curve varies with crystal anisotropy as we think, these low slopes would be expected. However, in some cases similar low values have been observed for the slope of strength vs. grain size curves for polycrystalline alumina so that present evidence is not sufficient to assert that the slope of the solid solution curve is less than that of pure alumina.

At larger grain size, other factors such as grain shape seem to have had a substantial influence on the results. For example, the average strength of specimens with a lath-like crystal structure from Billet 7-86 with an average grain size of 20 μm was 46,000 psi[21] whereas the strength of specimens with spheroidal grains and a bimodal grain size distribution from Billet 8-89-3 with an average grain size of 18 μm was only 24,100.

Estimating the Residual Stresses in Quenched Alumina Alumina from Mirror Dimensions

Evaluation of the results of this investigation should take into consideration the preliminary nature of the research which was performed mainly by analysis of specimens from other programs. In spite of this limitation,a wide range of relatively self consistent results were obtained. Therefore, this approach seems to have extraordinary promise for future research.

A good correlation between strength and mirror size was demonstrated. The slope of a log plot was 0.46 providing further evidence that the relation $\sigma_f r_m^{1/2}$ = constant is useful.

The residual compressive surface stresses estimated from strength vs. mirror size curves of specimens quenched into silicone oil (100 cs.) were as follows:

1550°C quenching temperature - 44,000 psi.

1700°C quenching temperature - 58,000 psi.

Fractures originating at internal flaws were investigated. Of particular interest was a fracture surface of a quenched specimen with a nominal flexural strength of 223,000 psi. This result is believed to be the highest flexural strength that has been obtained on a polycrystalline alumina rod. Also, when the alumina specimens failed at internal flaws, the strength and the location of the fracture origin were related, with the strength decreasing with increasing distance of the fracture origin from the rod axis.

At elevated temperatures, the mirror sizes in as polished rods are slightly smaller at a particular stress level compared with the sizes expected at room temperature. The value of $\sigma_f r_m^{1/2}$ was substantially higher than expected at 200°C. This variation should be investigated for evidence of factors affecting the fracture mechanism near this temperature.

The residual stress at the axis of alumina rods quenched from 1700°C into silicone oil (100 cs.) was estimated from the mirror sizes of rods that fractured spontaneously on reheating to 1100-1200°C. This residual tensile stress was about 76,000 psi. The estimated residual stresses were used to construct a residual stress profile. This profile was used to estimate the local stresses that caused failure in several quenched specimens that failed at internal flaws. These values decrease with increasing distance from the rod axis, a result foreshadowed by the similar variation of the strength. The location of the lowest local stress values corresponds approximately to the largest tensile stress gradient suggesting that other stresses play a role in these failures.

The most important result of this investigation is the observation that $\sigma_f r_m^{1/2}$ is approximately constant to temperatures as high as 1400°C. Since Young's modulus varies only slightly in this temperature range, this observation may indicate that the effective surface energy for fracture varies only slightly with temperature. If this is true it suggests that the contribution of microplasticity to the fracture energy is small. Further research should be done to investigate this possibility.

If it can be shown that microplasticity has only a minor role in the fracture of these brittle materials, it is necessary to look for new explanations of the variation of strength with flaw size. One possibility is that, even though a crack in a ceramic may be "atomically" sharp, it may act as though it is blunt because the interfacial forces reduce the stress concentration at the crack tip. It is frequently overlooked that the Griffith theory assumes that the surfaces are "traction free"[47]. Based upon experience with thermal expansion hysteresis and other phenomena in ceramics, it is apparent that these interfacial forces can be quite large so that it is reasonable to think that they may effect the fracture mechanism.

VI. REFERENCES

1. H. P. Kirchner, W. R. Buessem, R. M. Gruver, D. R. Platts and R. E. Walker, "Chemical Strengthening of Ceramic Materials," Ceramic Finishing Company Summary Report, Contract N00019-70-C-0418 (December, 1970).

2. H. P. Kirchner, R. M. Gruver and D. R. Platts, "Chemical Strengthening of Ceramic Materials," Ceramic Finishing Company Summary Report, Contract N00019-71-C-0208 (December, 1971).

3. R. W. Rice and W. J. McDonough, "Room Temperature Strength and Fracture Behavior of $MgAl_2O_4$," Paper No. 33-BN-71P, Fall Meeting, Basic Science Division, American Ceramic Society (November 3, 1971).

4. H. P. Kirchner and R. M. Gruver, "Strengthening Oxides by Reduction of Crystal Anisotropy," Ceramic Finishing Company Technical Report No. 5, Contract N00014-66-C0190 (April, 1971).

5. W. R. Buessem, "Internal Ruptures and Recombinations in Anisotropic Ceramic Materials," from "Mechanical Properties of Engineering Ceramics," Edited by W. W. Kriegel and H. Palmour III, Interscience Publishers, New York (1961).

6. W. R. Buessem and F. F. Lange, "Residual Stresses in Anisotropic Ceramics," Interceram 15 (3) 229-231 (1966).

7. F. J. P. Clarke, "Residual Strain and the Fracture Stress-Grain Size Relationship in Brittle Solids," Acta Met. 12, 139-143 (February, 1964).

8. D. P. H. Hasselman, "Single Crystal Elastic Anisotropy and the Mechanical Behavior of Polycrystalline Brittle Materials," from "Anisotropy in Single Crystal Refractory Compounds" Volume 2, Edited by F. W. Vahldiek and S. A. Mersol, Plenum Press, New York (1968).

9. H. P. Kirchner and R. M. Gruver, "Strength-Anisotropy-Grain Size Relations in Ceramic Oxides," J. Amer. Ceram. Soc. 53 (5) 232-236 (May, 1970).

10. J. S. O'Neill, N. A. Hill and D. T. Livey, "Observations on the Strength and Young's Modulus of BeO as a Function of Density and Grain Size," Proc. Brit. Ceram. Soc. 6, 95-101 (June, 1966).

REFERENCES (CON'T.)

11. G. G. Bentle and R. M. Kniefel, "Brittle and Plastic Behavior of Hot Pressed BeO," J. Amer. Ceram. Soc. 48 (11) 570-577 (November, 1965).

12. D. K. Smith, Jr. and S. Weissmann, "Residual Stress and Deformation in Extruded Polycrystalline BeO Ceramics," J. Amer. Ceram. Soc. 51 (6) 330-336 (June, 1968).

13. H. P. Kirchner, "Thermal Expansion Anisotropy of Oxides and Oxide Solid Solutions," J. Amer. Ceram. Soc. 52 (7) 379-386 (July, 1969).

14. H. P. Kirchner, R. E. Walker and D. R. Platts, "Strengthening Alumina by Quenching in Various Media," J. Appl. Phys. 42 (10) 3685-3692 (September, 1971).

15. H. P. Kirchner, R. M. Gruver and R. E. Walker, "The Strengthening of Polycrystalline Alumina by Crystalline Surface Layers," Trans. Brit. Ceram. Soc. 70 (6) 215-219 (September, 1971).

16. H. P. Kirchner, R. M. Gruver and R. E. Walker, "Strength vs. Grain Size of Pressure Sintered Alumina Strengthened by Quenching," Paper No. 41-BN-71P, Presented at the Fall Meeting, Basic Science Division, American Ceramic Society, (November 3, 1971); Submitted to J. Amer. Ceram. Soc.

17. L. R. Rossi and W. G. Lawrence, "Elastic Properties of Oxide Solid Solutions: The System Al_2O_3-Cr_2O_3," J. Amer. Ceram. Soc. 53 (11) 604-608 (November, 1970).

18. J. E. Hilliard, "Estimating Grain Size by the Intercept Method," Metal Progress 85 (5) 99-100 (May, 1964).

19. H. P. Cahoon and C. J. Christensen, "Sintering and Grain Growth of Alpha-Alumina," J. Amer. Ceram. Soc. 39 (10) 337-344 (October, 1956).

20. C. A. Bruch, "Sintering Kinetics for the High Density Alumina Process," Bull. Amer. Ceram. Soc. 41 (2) 799-806 (December, 1962).

21. H. P. Kirchner, R. M. Gruver and R. A. Ewig, "Strengthening Oxides by Reduction of Crystal Anisotropy," Ceramic Finishing Company Technical Report No. 3, Contract N00014-66-C0190 (April, 1970).

REFERENCES (CON'T.)

22. M. Hillert, "On the Theory of Normal and Abnormal Grain Growth," Acta Metallurgica 13, 227-238 (March, 1965).

23. R. M. Spriggs and T. Vasilos, "Effect of Grain Size on Transverse Bend Strength of Alumina and Magnesia," J. Amer. Ceram. Soc.46 (5) 224-228 (May, 1963).

24. R. J. Charles and R. R. Shaw, "Delayed Fracture of Polycrystalline and Single-Crystal Alumina," General Electric Research Laboratory Report 62-RL-3081M, (July, 1962).

25. L. A. Jacobson and L. L. Fehrenbacher, "Surface and Microstructural Influence on Flexure Strength of Dense, Polycrystalline MgO," Air Force Materials Laboratory TR-66-91 (May, 1966).

26. A. H. Heuer, "Transgranular and Intergranular Fracture in Polycrystalline Alumina," J. Amer. Ceram. Soc. 52 (9) 510-511 (September, 1969).

27. N. Terao, "Sur une Relation entre la Resistance a la Rupture et le Foyer d'Eclatement du Verre," J. Phys. Soc. Japan 8 (4) 545-549 (1953).

28. W. C. Levengood, "Effect of Origin Flaw Characteristics on Glass Strength," J. Appl. Phys. 29 (5) 820-826 (May, 1958).

29. E. B. Shand, "Breaking Stress of Glass Determined from Dimensions of Fracture Mirrors," J. Amer. Ceram. Soc. 42 (10) 474-477 (October, 1959).

30. E. B. Shand, "Breaking Stresses Determined from Fracture Surfaces," The Glass Industry, 190-194 (April, 1967).

31. J. W. Johnson and D. G. Holloway, "On the Shape and Size of Fracture Zones on Glass Fracture Surfaces," Phil. Mag. 14, 731-743 (1966).

32. M. J. Kerper and T. G. Scuderi, "Modulus of Rupture of Glass in Relation to Fracture Pattern," Bull. Amer. Ceram. Soc. 43 (9) 622-625 (September, 1964).

REFERENCES (CON'T.)

33. H. P. Kirchner, R. E. Walker and D. R. Platts, "Strengthening by Quenching in Various Media," J. Appl. Phys. 42 (10) 3685-3692 (September, 1971).

34. H. P. Kirchner, R. M. Gruver and R. E. Walker, "The Strengthening of Polycrystalline Alumina by Crystalline Surface Layers," Trans. Brit. Ceram. Scc. 70 (6) 215-219 (September, 1971).

35. H. P. Kirchner, R. M. Gruver and R. E. Walker, "Strength vs. Grain Size of Pressure Sintered Alumina Strengthened by Quenching," Paper No. 41-BN-71P Basic Science Div., American Ceramic Society Fall Meeting, November, 1971; Submitted to J. Amer. Ceram. Soc.

36. W. R. Buessem and R. M. Gruver, "Computation of Residual Stresses in Quenched Al_2O_3," J. Amer. Ceram. Soc. 55 (2) 101-104 (February, 1972).

37. J. Congleton and N. J. Petch, "Crack Branching," Phil. Mag. 8th Ser. 16, 749-760 (1967).

38. J. Congleton, N. J. Petch and S. A. Shiels, "The Brittle Fracture of Alumina Below 1000°C," Phil. Mag. 19 (160) 795-807 (April, 1969).

39. A. B. J. Clark and G. R. Irwin, "Crack-propagation Behaviors," Experimental Mechanics 321-330 (June, 1966).

40. R. H. Insley and V. J. Barczak, "Thermal Conditioning of Polycrystalline Alumina Ceramics," J. Amer. Ceram. Soc. 47 (1) 1-4 (January, 1964).

41. E. Ryschkewitch, "Oxide Ceramics," Academic Press, New York (1960).

42. A. G. Evans and R. W. Davidge, "The Strength and Fracture of Stoichiometric Polycrystalline UO_2," J. Nucl. Mat. 33, 249-260 (1969).

43. A. G. Evans, D. Gilling and R. W. Davidge, "The Temperature-Dependence of the Strength of Polycrystalline MgO," J. Mat. Sci. 5 (3) 187-197 (March, 1970).

44. A. G. Evans and R. W. Davidge, "The Strength and Oxidation of Reaction-Sintered Silicon Nitride," J. Mat. Sci. 5, 314-325 (1970).

REFERENCES (CON'T.)

45. R. W. Davidge and G. Tappin, "The Effects of Temperature and Environment on the Strength of Two Polycrystalline Aluminas," Proc. Brit. Ceram. Soc. 15, 47-60 (1970).

46. J. F. Lynch, C. G. Ruderer and W. H. Duckworth, "Engineering Properties of Ceramics," Battelle Memorial Institute Technical Report AFML-TR-66-52 (June, 1966).

47. A. A. Griffith, "Phenomena of Rupture and Flow in Solids," Phil. Trans. Roy. Soc. 221A, 163-98 (1920) p 166.